



Groundwater Flow Model of Corrective Action Units 101 and 102: Central and Western Pahute Mesa, Nevada Test Site, Nye County, Nevada



Revision No.: 0

June 2006

Prepared for U.S. Department of Energy under Contract No. DE-AC52-03NA99205.

Approved for public release; further dissemination unlimited.

Uncontrolled When Printed

8.3 Flow Model Sensitivity to Steady-State Temperature Distribution

8.3.1 Introduction

The Pahute Mesa CAU flow model spans an area 50 by 53 km with elevations between 3.5 km bmsl to 1.5 km amsl. Within the domain, there are three volcanic caldera complexes and extensive extra-caldera zones as well. Temperatures are not the same everywhere in this model domain.

In the flow model, spatial variations in temperature are set by specifying a steady-state, 3-D temperature distribution. The FEHM code accommodates changes in temperature through equations of state that relate viscosity and density to the specified temperature. Once set, however, the temperature distribution does not change over the course of a flow model or during flow model calibration.

The temperature field used in this study is derived from the calibrated, variable heat-flux model described in [Appendix C](#). In that model, heat fluxes at -3,500 m elevation are calibrated to minimize the difference between simulated and observed temperatures in boreholes in the model domain. However, most of the temperature measurements are in the upper one-fifth of the model domain, leaving uncertainty in temperatures and, hence, water properties at depth in the model.

An alternative to simulating a temperature field, as described in [Appendix C](#), is to simply specify a fixed geothermal gradient. Such an approach can match observed temperatures reasonably well if it is anchored to observations and extrapolates temperatures at depths below where the observations occur. Therefore, the thermal sensitivity here involves specifying temperatures at all depths in the model domain to correspond with thermal gradients of 10 degrees per kilometer ($^{\circ}/\text{km}$) and $30^{\circ}/\text{km}$, representing low and high gradients for the system ([Appendix C](#)). The thermal fields for these sensitivity runs are anchored to the observed temperature of 47.7°C in Well ER-20-05 #3 at an elevation of 656.5 m amsl. Starting with the calibrated parameters for the BN-MME-SDA flow model, the temperature distribution is changed to reflect the low and high linear geothermal gradients. The flow model is not recalibrated and forward simulations are compared with the base-case model.

8.3.2 Sensitivity Results

For both the 10°/km and the 30°/km linear thermal gradient temperature fields, the model objective function increases from the calibrated model. [Figure 8-5](#) shows the components of the objective function for each of the models considered. With the linear thermal gradients, temperatures at depth are greater than those computed with the heat conduction model. Thus, for the same permeability, hydraulic conductivity at depth increases. With increased hydraulic conductivity at depth, flow increases at greater depths, ET discharge in Oasis Valley decreases, and heads in shallow HSUs decrease.

It is interesting to note that although heads and fluxes in the sensitivity simulations change from those in the base model, simulated pathlines are about the same. [Figure 8-6](#) shows forward paths originating at wells and reverse-particle exit locations for ER-OV-04a for the two thermal sensitivity runs. There is virtually no difference between the runs and they are nearly identical to the results shown in [Figure 7-19](#) for the calibrated flow model with variable heat-flux-based temperatures. Quantitatively, the fractions of 10 million particle exits in the different source zones are nearly identical as well. This result holds for all eight of the geochemistry target wells considered.

8.3.3 Summary of Thermal Sensitivity Results

For all flow models used in this analysis, the temperature distribution resulting from the calibrated, variable base-flux conduction model is used. Here, as part of an assessment of model sensitivity to temperature, two different temperature distributions based on linear thermal gradients and extrapolation from a high-quality measurement are considered. It is not surprising that the model objective function increases with the two sensitivity runs because these fields are different than that used for calibration. The increased temperature at depth results in greater hydraulic conductivities for the same permeability developed in the calibrated base model. Thus, it is likely that the objective function could be reduced through calibration. It is possible that reasonable calibrated permeability fields could be achieved with linear thermal gradient. To offset the higher viscosities, lower rock permeabilities would be computed. However, it is unlikely that linear thermal gradients would lead to as good or better results than those achieved with the calibrated thermal field, which captures non-linear distributions of rock properties

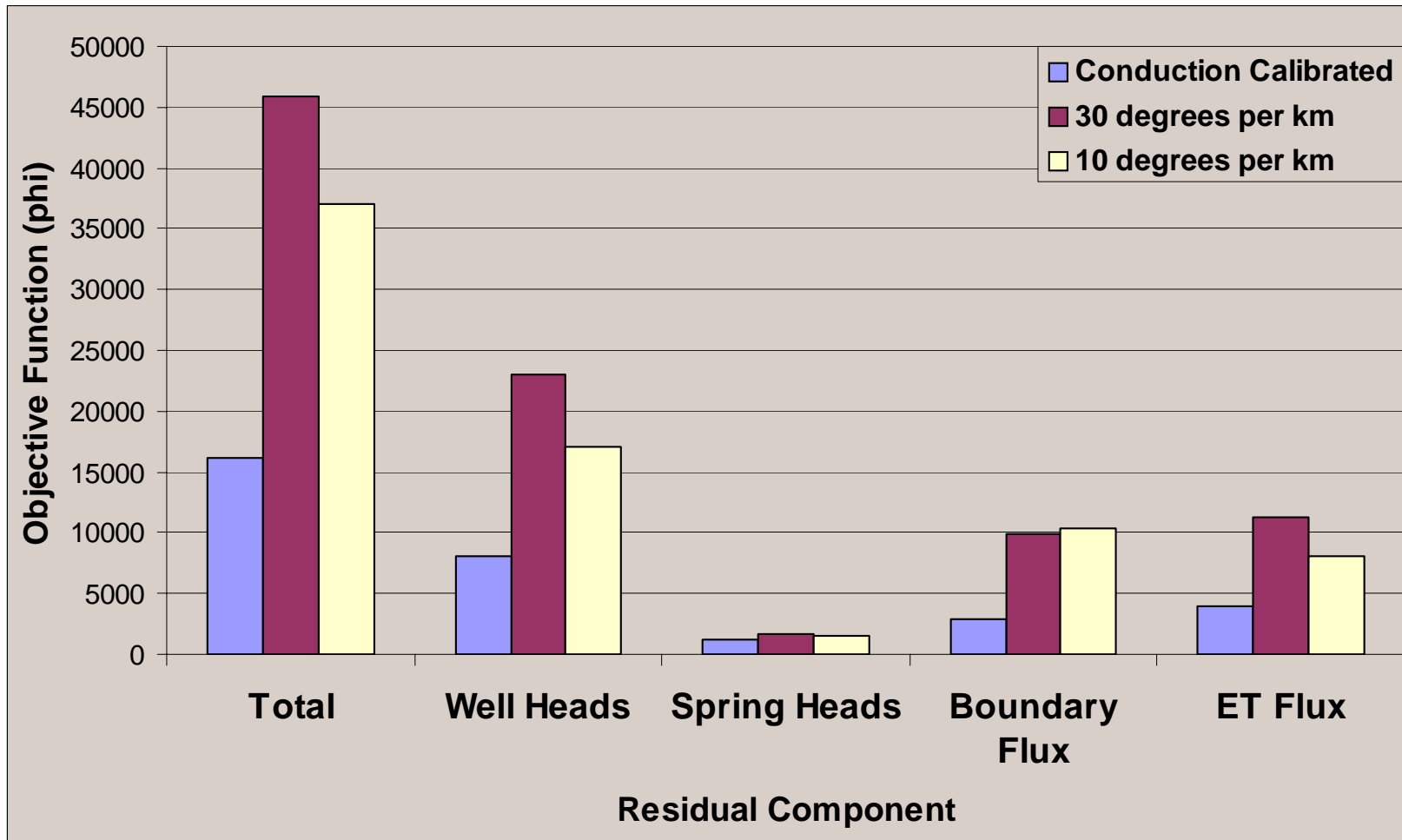


Figure 8-5
Comparison of Flow Model Objective Functions for Different Thermal Fields

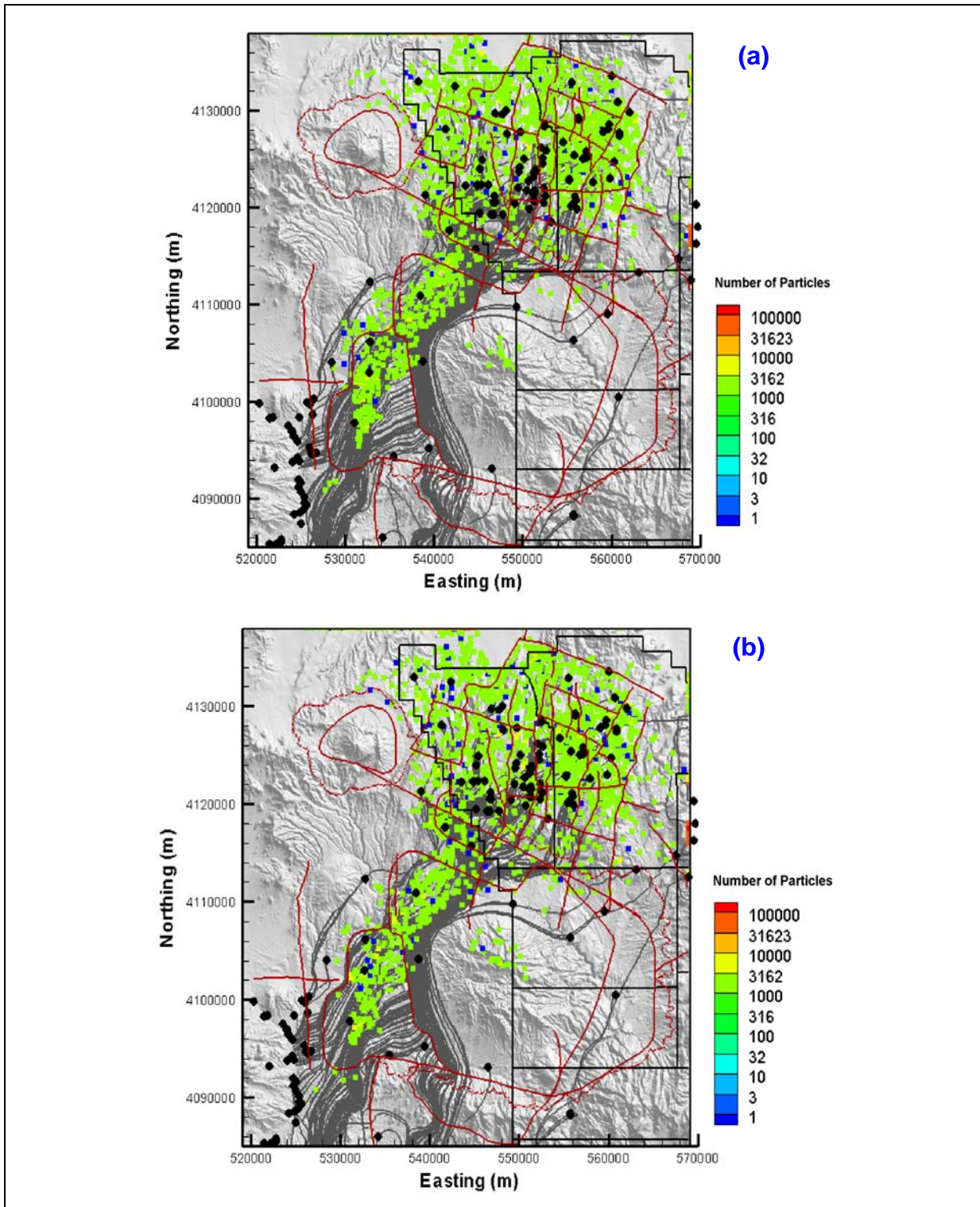


Figure 8-6
Comparison of Forward Flow Paths (Grey)
and Reverse-Particle Exits from ER-OV-04a
(a) the 10°/km Thermal Sensitivity Run (b) and the 30°/km Thermal Sensitivity Run

A curious result in this sensitivity analysis is that even with poorer matches to head and flux, the pathlines and reverse-particle-tracking simulations are nearly identical for the base model and the two thermal sensitivity runs. This is likely due to the fact that the models are most similar at the shallower depths where the forward particles are introduced. Recharge also enters the model at the shallower depths and is the same for each of the models. Thus, the reverse particles are likely to exit at the locations where recharge occurs.

9.0 SUMMARY AND CONCLUSIONS

To understand the potential for lateral and vertical radionuclide migration, a 3-D, finite element, steady-state groundwater flow model of the Central and Western Pahute CAUs was constructed. The model was created to allow for evaluation of conceptual model uncertainty. Different combinations of HFMs, recharge models, hydrologic boundary conditions, and application of permeability depth decay were considered in order to propagate the uncertainty associated with each of these elements of the model into the resulting flow fields. The approach resulted in several flow fields that were consistent with site-specific data and the conceptual understanding of the Pahute Mesa groundwater flow system. The modeling effort was able to synthesize an understanding of the regional hydrogeologic system and local data and observations while bounding flow-field uncertainty resulting from geologic and hydrologic uncertainty. This analysis was undertaken to satisfy the groundwater flow model required by the *Corrective Action Investigation Plan for Corrective Action Units 101 and 102, Central and Western Pahute Mesa, Nevada Test Site, Nevada* (DOE/NV, 1999).

Pahute Mesa is located in the northwestern part of the NTS; it includes NTS Areas 19 and 20. Pahute Mesa is an elevated plateau of about 500 km² (200 mi²) at an altitude that ranges from 1,676 m (5,500 ft) on the western edge to over 2,134 m (7,000 ft) amsl throughout the eastern range (Blankennagel and Weir, 1973). The area of interest for the Pahute Mesa CAU is defined by the potentially affected portion of the regional groundwater flow system from the 82 underground nuclear tests conducted on Pahute Mesa, which includes a region stretching from the northern side of Pahute Mesa south and southwestward towards Oasis Valley.

Pahute Mesa geology is dominated by deposition of rock units from volcanic eruptions from nested calderas of the SWNVF. All rocks known to underlie Pahute Mesa are volcanic. The youngest caldera complex of hydrologic significance is the Timber Mountain Caldera. This caldera collapse and its filling with volcanic materials resulted in volcanic ash flows covering much of Pahute Mesa to the north. On Pahute Mesa, the rocks from Timber Mountain Caldera cover an older series of calderas that make up the SCCC. This caldera complex consists of at least two nested calderas, the

Area 20 Caldera and the older Grouse Canyon Caldera. Both calderas were formed and subsequently filled by voluminous eruptions of tuff and lava of generally rhyolitic composition. Total thickness of volcanic rocks beneath Pahute Mesa is on the order of 5 km (16,000 ft).

Groundwater beneath Pahute Mesa generally flows in a southwest direction, primarily through fractures in the lava-flow and tuff aquifers. Zeolitized bedded and nonwelded tuffs act as confining units that inhibit the flow of groundwater. The spatial distribution of permeable aquifers relative to the confining units is not well understood. Thickness variations of aquifers and confining units and their connectivity across faults or caldera boundaries are important hydrostratigraphic relationships that are also not well understood. A number of wells provide water-level information in the Pahute Mesa and Oasis Valley areas, but water levels in the area between Pahute Mesa and Oasis Valley are less well defined. However, what data are available suggest that groundwater elevations gently mimic the topography. Groundwater elevations are highest beneath northern Pahute Mesa, ranging in elevation from approximately 1,280 to nearly 1,500 m (~4,200 to 4,900 ft), with the depth to water on average of about 600 m (~2,000 ft). Groundwater elevations drop off gradually to the south and west, ranging from 1,100 to 1,250 m (~3,600 to 4,100 ft) in Oasis Valley. Some groundwater discharges to the surface within the Oasis Valley discharge area in the form of springs.

Groundwater recharge occurs locally from precipitation from areas located to the north of Pahute Mesa. Groundwater then flows south-southwestward to the Oasis Valley and Death Valley to the southwest. Several factors are believed to account for the flow around Timber Mountain. Due to its elevation, Timber Mountain receives more precipitation compared to surrounding areas of lower elevation, which leads to additional groundwater recharge at Timber Mountain. In addition, extensive zeolitization and clay alteration of the tuffs within the Timber Mountain Caldera causes these volcanic units to behave more like confining units than aquifers. Both of these factors are expected to lead to a mounding of the groundwater levels beneath the mountain, which affects groundwater flow paths from Pahute Mesa such that they would go around both sides of Timber Mountain rather than directly through the caldera.

The foundation of the flow model analysis is the Phase I HFM prepared and documented by BN (2002). The base (or BN) HFM incorporates all of the geologic data and evaluations deemed to provide the most viable interpretation of the hydrogeologic system. An additional major alternative

interpretation is the structurally uncoupled variant termed the SCCC. Major structural differences with the BN HFM include the margins of the caldera complex (single caldera ring-fracture system), locations of caldera-forming faults, and the number and depth of faults. To investigate the uncertainty in the BN HFM, five alternative geologic models were developed to assess the potential impact of alternative geologic interpretations on groundwater flow and the transport of contaminants in groundwater. The DRT alternative projects the Belted Range thrust LCCU1 through the model to the west. Effects of the TCL were developed by substituting more fractured rock HSUs. The depth of the basement rocks has an uncertainty of 2,000 m; the raised PZUP alternative brought the Paleozoic rocks to as high an elevation in the HFM as permitted by the drill-hole and geophysical data under the entire flow model area. An alternative geologic interpretation that attempts to account for the geophysical gravity anomaly between the Timber Mountain and Silent Canyon Calderas southwest of Area 20 was developed in the RIDGE alternative. Representation of the Paleozoic rocks as a continuous sheet in the southeast model domain was incorporated in the SEPZ alternative. Each of these HFMs was evaluated to determine uncertainty in the calibrated flow field of the BN HFM.

The hydrostratigraphy was translated into a computation model via finite-element meshes for use with the FEHM code to capture the complex HSU geometries and faults, and test chimneys for the two major HFMs: the BN base and SCCC. The mesh node spacing ranged from 67.5 m to 1 km, with refinement in thinner HSUs, around tests, and estimated flow paths from Areas 19 and 20 to Oasis Valley. About (depending on HFM) 46 HSUs and 37 faults are represented in the models. This resulted in two meshes with approximately 1.4 million and 1.3 million nodes for the BN and SCCC HFMs, respectively. The model area is 53.4 km (33.2 mi) north to south and 50.8 km (31.6 mi) west to east.

Once the meshes were constructed, heads interpolated from the UGTA regional model were assigned to the edges of the CAU as boundary conditions, and inside the CAU model as initial conditions. The calibrated thermal fields (see [Appendix C](#)) were specified as a fixed condition; that is, thermal transport was not simulated but the variable temperature field was specified. Five recharge models were prepared as input to investigate water-balance uncertainty: two based on the chloride mass-balance (called the DRI models) analysis of Russell and Minor (2002), one based on the modified Maxey-Eakin (MME) empirical approach developed for the UGTA regional model (DOE/NV, 1997), and two based on the distributed parameter model (called the USGS models) of

Hevesi et al. (2003). The USGS models had the lowest recharge flow, the DRI models the highest, and the MME model was intermediate between the USGS and DRI models.

Calibration data for well and spring head as published by SNJV (2004a) were assigned to the appropriate model nodes. In addition, Oasis Valley discharge as estimated by Laczniak et al. (2001) was represented by third-type boundary conditions in order to provide a flow constraint internal to the model. Flow on the CAU model edges was also output by FEHM and compared to the UGTA regional model. Thus, four datasets were used to calibrate the model: well head, spring head, Oasis Valley discharge, and UGTA regional model boundary flow. The goodness of the flow model is enhanced by considering these different types of data, especially flows (Hill, 1998). In particular, matching both head and flow in Oasis Valley increases confidence that the model behavior is correct in this area. A total of 191 calibration targets of head and flow were used in the model calibration. Once the necessary input and calibration data were mapped onto the model meshes, the files for the parameter estimation program PEST were created, and flow model calibration began.

Flow model calibration followed a generally accepted protocol in which model parameter sensitivities to calibration were evaluated and interpreted in light of the conceptual model of the system. The parameter estimation program PEST was used to streamline this process, providing sensitivity coefficients, model parameter correlation coefficients, and eigenvalue and eigenvectors. Discrete parameter changes were also investigated during the calibration process. In general, not all parameters that were sensitive were adjusted during calibration based upon their uncertainty. Parameters that were highly correlated were removed from the calibration process. A further constraint was the desire to honor, within the range of uncertainty, the estimated hydraulic properties for HSUs. Weights reflecting the uncertainty in the calibration target data were initially developed and then re-evaluated based on judgment about the importance of matching the type of data. Thus, the Oasis Valley discharge and UGTA regional model boundary flow weights were increased because it was judged important to match discharge to Oasis Valley (the closest biosphere access to source locations) and to honor the estimated regional water balance on the model domain (a particularly important constraint considering the model is mostly surrounded laterally with constant heads).

The starting point for the CAU model specified-head boundary conditions was the UGTA regional model results interpolated onto the mesh edges. Changes were made during calibration to address

inconsistencies to measured heads in the following areas: western part of the northern boundary, the north-central model edge near UE-20p and PM-2, southern edge of the model east of Oasis Valley, and eastern boundary near TW-1. Also, the northwest corner of the model (both north and west faces) was converted to a no-flow in conjunction with correction of heads in the vicinity of PM-2 and UE-20p.

A variety of parameterization approaches have been used to simulate groundwater flow in the NTS area (e.g., the UGTA regional model [DOE/NV, 1997], the USGS flow model of D’Agnese et al. [1997], and the YMP saturated-zone model [DOE/ORD, 2004]). The viability of four different parameterization approaches was tested: (1) no anisotropy and no depth decay of HSU permeability, (2) depth decay applied to selected HSUs, (3) anisotropy and depth decay applied to selected HSUs, and (4) anisotropy and depth decay applied to all HSUs. Approach (1) is a limiting case of simplicity; approaches (2) and (3) reflect parts of the USGS regional model (D’Agnese et al., 1997), the DVRFS model (Belcher et al., 2004), and the YMP saturated zone models (DOE/ORD, 2004); and approach (4) reflects the same approach used in the UGTA regional model. The BN HFM with MME recharge was calibrated with the four parameterization approaches above. The MME recharge model was selected because its value was in between the USGS and DRI models, and thus was approximately the central tendency of the recharge models. The no-anisotropy and no-depth-decay case was rejected as a reasonable approach because flow paths from Pahute Mesa tended to dive deep below Oasis Valley, reflecting the poor match of Oasis Valley discharge data. The selected HSU depth decay with no anisotropy was investigated briefly, but completely neglecting anisotropy was deemed unreasonable, and it was discarded. The application of anisotropy and depth decay to selected HSUs and to all HSUs approaches were carried to a final calibration. Both calibrated models could represent the flow system reasonably well, as defined by matching calibration targets. In addition, the SCCC HFM with MME recharge with the selected HSU anisotropy and depth-decay approach was also calibrated. This HFM did not calibrate as well as the two models calibrated using the BN HFM.

The change in observed hydraulic head over the Pahute Mesa CAU flow model is nearly 600 m. In general, the trend of model simulated and observed head is reasonable, however, there are a few areas of increased local error in all models. The SCCC HFM showed larger errors than the BN HFM.

The discharge in Oasis Valley was matched within one standard deviation of the estimated value by the BN-MME-SDA and BN-MME-ADA models, and not quite within one standard deviation by the SCCC-MME-SDA model. However, all models showed a mild spatial bias in discharge error with the highest flow at the northern end of Oasis Valley being reasonably matched with significant under simulation of flow for ET Zones 3 (located in the northwest part of Oasis Valley, see [Figure 4-17](#)) and 5 (in the central part of Oasis Valley, see [Figure 4-17](#)) in all cases. Thus, while the total Oasis Valley discharge is reasonably matched, it appears that some feature in either the HFM or the boundary condition itself needs refinement to better capture the spatial distribution of Oasis Valley discharge.

The UGTA regional model estimated boundary flows were also reasonably matched; the sense of the flow (e.g., in or out) was usually correct, and the error was typically within 20 percent. Thus, the general flow of water is in broad agreement with the regional understanding of the flow system. As an additional check on the CAU water balance the flow along the northern edge of the Yucca Mountain saturated zone model, which lies entirely within the Pahute Mesa CAU flow model, was compared to the CAU model results. The YMP saturated zone model (DOE/ORD, 2004) gives a value of 196 kg/s inflow. The calibrated models give values of 250, 300, and 218 kg/s for the BN-MME-SDA, BN-MME-ADA, and SCCC-MME-SDA cases, respectively. The DVRFM (Belcher et al., 2004) boundary flows were also estimated (see [Table 5-5](#)) for the Pahute Mesa CAU flow model, and were within the ranges developed from the UGTA regional model.

The BN and SCCC HFMs showed markedly different behavior along the Purse Fault, where a 100-m head discontinuity has been observed. The BN model has a long and deep representation of the Purse Fault, whereas the SCCC has a short and shallow Purse Fault representation. Thus, it is incapable of serving as a nearly impermeable barrier in the SCCC HFM between the northwest quadrant and the north-central portion of the model. This difference allowed the BN HFM to better represent the change in water levels across the fault. Juxtaposition of HSUs across the fault is incorporated in both HFMs; thus, the arrangement of HSUs alone is insufficient to capture the fault behavior.

At the Boxcar Faults, the BN and SCCC HFMs performed similarly. With a higher head to the east of the fault, a lower permeability is required along the fault itself to replicate the observed head drop, and both models improved as the fault permeability decreased. Wolfsberg et al. (2002) also noted

similar model behavior for the Boxcar Faults in their groundwater flow model of the area surrounding the TYBO and BENHAM underground nuclear tests.

Comparison of the calibrated permeabilities to those from single-well constant-rate tests showed a bias toward lower calibrated permeabilities. This is not unreasonable, because tested zones in fractured rock are those that typically have higher permeabilities while the model incorporates the entire thickness of rock. In addition, it has been shown that effective properties of a porous medium, especially permeability, decrease with the scale of analysis (Neuman, 1990); the so-called “scale effect.” With the exception of ER-20-6 #1 and ER-20-6 #2, all the tests were single well, which would tend to have a relatively small sampling radius. Slug tests were not considered in this comparison because they are strongly affected by near-well mechanical disturbance (e.g., drilling) (Butler, 1997) and have an even smaller sample volume than single-well tests. Finally, the approach taken (and described in the Pahute Mesa CAIP [DOE/NV, 1999]) in parameterizing HSUs for the HFMs was to avoid specifying many small patches of different properties, but rather to use broad zones of constant properties that were developed from characterization data. Any individual test describes only a small volume of the zone in which it lies; thus, some misfit must be tolerated because the data density does not allow anything but a broad description of HSU properties.

The range of permeabilities estimated in the Pahute Mesa hydrologic data document (SNJV, 2004a) for the TMA, TCM, PCM, YMCFCM, PBRCM, and LCA are compared to the ranges in the model, and are generally in reasonable agreement. The range of PCM permeabilities used in the models matches the estimated range well; the LCA less so, being biased low. For HSUs on Pahute Mesa, the KA, CHVTA, CHVCM, CFCU, and BFCU model-calibrated values are very similar to the estimated mean. The IA is about an order of magnitude lower than expected. The calibrated permeabilities for CHZCM, CFCM, and CHCU are toward the lower end of uncertainty (close to two orders of magnitude lower than the mean). Composite units are a mixture of HGUs, and because homogeneous parameters were used for these HSUs, it may be the heterogeneity of the HSU causing this variance. The THLFA, THCM, LPCU, TCA, PLFA, and FCCU all are close (less than half an order of magnitude variation) to the expected mean. The BA is close to the mean for BN-MME-SDA but an order of magnitude lower for SCCC-MME-SDA because it also includes the UPCU. The TSA has the greatest fluctuation among HFMs. The UPCU for BN-MME-SDA is about two orders of magnitude lower than the mean. The FCA, YVCM, DVCM, LCCU1, and PVTA are close (within a

half an order of magnitude), while FCCM and DVA are about an order of magnitude lower than expected. The AA and UCCU are lower than even the lower limit by 2 and 1.5 orders of magnitude, respectively. The estimated mean permeability for the UCCU of $3.7 \times 10^{-13} \text{ m}^2$ seems somewhat high, and is based on two data points (see Figure 5-22 in SNJV, 2004a).

After calibration a formal sensitivity analysis was conducted. The sensitivity analysis used local techniques (all parameters are perturbed slightly or one at a time over their range of uncertainty) and global techniques (considered effects of joint parameter uncertainty over full range of uncertainty). The local approach used PEST to identify sensitive model parameters, sensitive observations, and parameter correlations. The perturbation analysis varied properties of HSUs and faults over their range of uncertainty, providing a comprehensive picture of model behavior (although without considering compensating effects). Major faults often showed a one-sided sensitivity behavior, where fault permeability multiplier ceased to have a noticeable effect below a certain value. The Purse Fault permeability multiplier, for instance, could be as high as 0.001 (that is, the fault permeability is 1,000 times less than the surrounding rock) before much model misfit was noticed – behavior that was similar in the BN HFM with depth decay applied to all HSUs (ADA) and only to selected HSUs (SDA). This behavior was not noticed in the SCCC HFM because the Purse Fault is not as long or as deep.

Global sensitivity analysis was conducted by generating 1,000 uncorrelated flow model parameter samples using Latin Hypercube sampling, computing flow model results for these samples, and recording the model results for the two calibrated versions of the base HFM (all and selected HSU depth decay and anisotropy) and SCCC HFM. This approach was taken to attempt to identify whether there were parameter combinations that were as good or better in calibrating the model than the chosen sets over the range of parameter uncertainty, and whether there were systematic effects of some model parameters. The results were analyzed using Spearman rank correlations, classification and regression trees, and entropy statistics. Similar sets of sensitive variables were identified in the local and perturbation analyses, notably the control of the PCM on model head and the DVCM on Oasis Valley discharge.

These sensitivity analyses led to the following findings:

- The PCM, YMCFCM, CHCU, and DVCM HSUs; and the Claim Canyon Caldera Structural Margin fault (fault 06 in the BN and fault 03 in the SCCC) were sensitive in controlling heads in the BN and SCCC HFMs. For the PCM and YMCFCM, this is because they are astride the southern boundary and control the influence of the strong head drop (observed regionally and incorporated in the CAU model) at the southern edge of the CAU model. Similarly, the Claim Canyon Caldera Structural Margin fault is convex open to the north with its apex at the southern boundary, which controls flow to the south. Finally, the DVCM is located in the southwest corner of the domain along the southern part of the western edge and western part of the southern edge, and controls both in and outflow to Oasis Valley. The CHCU controlled heads in the BN-MME-ADA case because of its location in an arc around the Silent Canyon Caldera structural margin causes it to act as a dam controlling head propagation west of the Greeley faults. In the SCCC, all the Calico Hills units were lumped into the CHCU (a model naming convention only; the unit was not parameterized as a confining unit), the properties of which are the effective properties of the combined BN Calico Hills units. In the SCCC HFM CHCU is several hundred meters thick and has many head observations, hence the model sensitivity.
- The thrust LCCU, the LCCU1, controlled heads in the HFMs at higher permeabilities due to its connection to high heads along the northern part of the eastern edge (e.g., west of Rainier Mesa). The properties of this unit are not well known, the single test value is relatively high and may be biased (only permeable intervals are readily tested). The conceptual model of this unit is that its permeability is ubiquitously increased due to deformation from thrusting stresses.
- Reference permeability and depth decay have a nearly perfect correlation, which is expected considering the formulation of depth decay.
- Over their range of uncertainty, the reference permeability of HSUs with depth decay was more sensitive than the depth-decay parameter itself. It is important to note that this was recognized during calibration, and depth-decay coefficients as estimated for each type of HSU (e.g., volcanics and carbonates) were fixed and reference permeability calibrated; it is poor practice to attempt to adjust strongly correlated parameters simultaneously.

Perturbation analysis on HSUs localized on Pahute Mesa for the BN-MME-SDA case showed that the BFCU, IA, CHZCM, and TCA had noticeable control on model results over their estimated range of permeability uncertainty. The IA has no wells with calibration data in it, but the model is sensitive to its permeability probably because of its larger extent (relative to most other HSUs on Pahute Mesa) extent and complex connection to the CHZCM, which has head data for calibration. Several HSUs had practically no effect on model results because of the lack of calibration data, geometric isolation

or discontinuity, or small saturated extent including: KA, CFCM, CFCU, TSA, LPCU, PLFA, UPCU, BA, and PVTA.

Model calibration and sensitivity analysis revealed that at higher permeabilities the LCCU1 (thrust LCCU relatively high in the geologic section on the northeastern edge of the HFM) routes pressure and flow into the domain exerting noticeable control on model results. The conceptual model of the LCCU1 is that thrusting stresses have ubiquitously enhanced its properties (SNJV, 2004a), which may be overly simplistic. Caine et al. (1996) studied a slip fault exposure in Paleozoic clastic rocks and found that where the rock was predominantly shale, the fault core lithology was dominated by clay-rich gouge with a localized damage zone that acted both as barrier and conduit features, respectively. The total fault zone width was only a few meters. Seaton and Burbey (2005) investigated a thrust fault and found that the fault plane itself had low permeability, and that the highly fractured zone (up to 10 m thick) was localized above the fault plane. Seaton and Burbey (2005) studied crystalline rocks in the Blue Ridge province of Virginia, and this observation may not be directly extensible to the sedimentary rocks of the NTS. However, a plausible conceptual model of the LCCU1 may be generally low permeability along the plane of the thrust fault and in undisturbed low-permeability rocks with thin zones of enhanced permeability from fracturing adjacent to the thrust plane, which would reconcile both the single hydraulic test result and model behavior.

Only three HSUs under Pahute Mesa were identified by the local and global sensitivity analyses as having ubiquitous influence on model calibration statistics: the PBRCM, BRA, and CHCU. These HSUs are extensive in area relative to most of the HSUs on Pahute Mesa proper, and to some degree, the sensitivity of model results to their permeability is probably related to their continuity and their updip extension to the water table. For instance, the CHCU has a relatively large areal extent and separates shallower volcanic HSUs (where much of the calibration data exist) from the deeper PBRCM and BRA. The DVCM also had ubiquitous influence on model results because of its control on flow into Oasis Valley from Sarcobatus Flat.

A set of discrete sensitivity analyses was also considered including the following: testing the effects of permeability enhancement of test chimneys; evaluating the effects of two additional plant rooting depths, or depth from which water can be transpired from the water table, on Oasis Valley discharge;

considering the effect of a reduced LCCU1 permeability alternative (suggested by the sensitivity analysis); and testing the consequences of trying to enhance flow down Fortymile Canyon. The effects of test chimneys were found to be negligible; the simulated Oasis Valley flows were mildly sensitive to the rooting depth, the model could still be calibrated well with lower LCCU1 permeability alternative, and enhancing flow down Fortymile Canyon does not look feasible.

The complexity of the geology in the area, and the resulting uncertainty in geologic interpretation, was addressed by the development of alternative framework models based on the BN HFM, and by quantitatively evaluating these alternative HFMs with FEHM. The flow models were calibrated for each of these alternative HFMs and the MME recharge model. Thus, the high-level uncertainty in geologic structure is addressed. Of the five alternatives, three (TCL, RIDGE, and SEPZ) required no additional effort over the base BN HFM to recalibrate, although the calibrations and simulated flow paths did show some differences. Two alternatives (DRT and PZUP), both involving raising or otherwise increasing the amount of low-permeability rocks in the domain, required extensive effort to recalibrate. The calibration process resulted in metrics similar to the base BN HFM calibration, with some modest changes in simulated flow paths.

Another component of model uncertainty is that associated with the water balance, which directly controls the flow rate (and hence velocity) of water through the domain. Having held the recharge model constant (MME) and changed HFMs, the opposite approach of using the BN and SCCC HFMs with alternative recharge models and associated boundary flows was also used. The base HFM (with anisotropy and depth decay applied to selected HSUs) was recalibrated using the two USGS and two DRI recharge models. The results were very similar between pairs of models (e.g., USGS with and without runoff). The USGS recharge model with run-on and runoff (USGSD) is conceptually more reasonable, so it was retained for further analysis. Likewise, the DRI recharge model with alluvial screen (DRIA) was retained because it has the highest flow rates and should bound the upper end of flow through the system. Thus, the SCCC HFM was tested with the DRIA and USGSD recharge models only. The USGSD recharge model provided some of the best calibrations, with the DRIA recharge giving results similar to or worse than the MME recharge models. The most noticeable effect was that flow paths in the SCCC HFM changed with different recharge models such that more paths were directed down Fortymile Canyon.

The final phase of uncertainty analysis was to combine HFM and recharge model uncertainty. This was accomplished by taking the alternative HFMs most different than the base (the DRT and PZUP HFMs) and analyzing them with the USGSD and DRIA recharge models. The PZUP HFM calibrated poorly with the USGSD recharge map because the increased volume of low-permeability rock and low recharge made it difficult to get enough water in the domain resulting in systematic under simulation of water levels. However, because the error was systematic, the flow directions remained very similar to other recharge models. The DRT HFM could be calibrated to similar degrees as other models, although superior to the PZUP under the USGSD and DRIA recharge models. The DRT HFM, under all recharge conditions, simulates a focused flow path around the northern edge of Timber Mountain at the highest consistent elevations (~1,100 m [~3,600 ft]) in the flow system. All the HFMs show such a path, but the DRT HFM shows the greatest concentration of flow lines in this area.

The Pahute Mesa CAIP states that flow model verification will be conducted (DOE/NV, 1999). Because of head data sparseness, no head or flux information was held out of the calibration for later use in verification (as described in the Pahute Mesa CAIP [DOE/NV, 1999]). However, Kwicklis et al. (2005) analyzed geochemical signatures of various waters in the area and generated mixing targets at key points in the model domain that were used for model verification. A reverse-particle-tracking methodology was developed that allowed identification of the sources of water at eight target wells for comparison to geochemical estimates. These estimates were used for geochemical flow model verification. Nineteen alternative models were tested with the geochemical mixing targets. The target wells at the higher parts of the flow system were more difficult to match because there is less distance for mixing to occur, and very complex flow paths (at ER-EC-6, for instance) produce poor comparisons because of narrow flow path deviations. In general, the geochemical trends are captured.

Cluster (K-means) analysis of the geochemical verification results was used to further group the combinations of calibrated HFM and recharge models. Four clusters resulted with four, four, five, and six flow models in the ranking of worst to best clusters. The best cluster of calibrated models with respect to the geochemical verification included the DRT HFM with MME and DRIA recharge models, the reduced LCCU1 alternative with the MME and USGSD recharge models, the PZUP HFM with the MME recharge model, and the SCCC HFM with the MME recharge model. The eight

models in the two worst clusters are judged to be in direct conflict with the interpreted geochemistry, and are to be eliminated from further consideration in future transport analyses. The remaining cluster of five calibrated models has less severe problems than the worst two clusters, and for some metrics even performs better than the best cluster. These models will be considered in less detail during transport calculations, perhaps in sensitivity analysis.

Thermal analysis was also used as a qualitative test of model consistency. Thermal analysis suggested areas where flow of cooler water downward could explain temperature anomalies. Reverse-particle tracking was conducted at the four locations of cooler thermal anomalies to test whether simulated flow paths were such that cooler water from upgradient could be seen to flow to the well. The results used the BN-MME-SDA reduced LCCU1 permeability alternative were positive with the model simulating such flow paths.

Bredehoeft (2005) suggests that selecting the proper conceptual model (that is, addressing conceptual model uncertainty) is a major problem in groundwater modeling analysis. He suggests that this can be overcome by collecting as much data as feasible using all applicable methods, and by leaving the conceptual model open to change. Recently, Nishikawa (1997) and Harrar et al. (2003) present analyses where alternative geologic conceptual models are tested in simulating groundwater flow and transport results. Nishikawa (1997) found that some conceptual alternatives better explained reality, while Harrar et al. (2003) found that while all the alternative models could replicate the calibration data, their performance in predicting capture zones and breakthrough were quite different, and inverse modeling coupled with alternative geologic models (such as that described in this report) could be used to assess predictive uncertainty. A total of 26 individual flow model calibrations for the Pahute Mesa CAU, and geochemical verification of most of them, were conducted and are presented in this report. These calibrations reflect a variety of combinations of alternative HFMs, recharge models, and water-balance conditions. Thus, the approach taken for the Pahute Mesa flow model attempts to bound the proper conceptualization of HFM and water balance, and at least addresses the high-level uncertainty associated with the conceptual model.

The Pahute Mesa CAU flow model is calibrated to hydraulic head and estimates of boundary flow and Oasis Valley discharge. This information is utilized to give the direction and velocity of groundwater flow, which will be used to compute contaminant transport in conjunction with the

appropriate processes (e.g., advection, dispersion, retardation, and radioactive decay). However, the solute transport process has profoundly different characteristics than groundwater flow alone (Anderson, 1979). Mathematically, the steady-state saturated groundwater flow equations are elliptic, with smoothly varying head, while the solute transport equations range from parabolic (with smoothly varying concentrations) in the case of dispersion-diffusion dominated system to hyperbolic (with sharp concentration fronts) in the case of advection-dominated systems. Consequently, calibration to head and flow does not necessarily inform or constrain solute transport. Thus, there may be additional uncertainty associated with the flow model when it is used to make predictions of radionuclide transport. The effects of concentration data on flow model calibration were examined by Weiss and Smith (1993 and 1997). They examined how head and concentration data interact in model calibration with eigenspace and response surface analysis. They showed that, depending on the flow model structure, concentration data could range from being unbeneficial to very beneficial in supplying additional flow model constraint. Scheibe and Chien (2003) showed that calibration of a flow and transport model with a large number of small-scale measurements of concentration and formation properties does not necessarily yield improved predictions, but that broader scale data do. Thus, simply collecting radionuclide or other concentration data does not guarantee improved transport predictions; the data must be collected with an understanding of how the hydrogeologic system (represented by the model) behaves.

The FFACO (1996) requires that the contaminant transport model predict the contaminant boundary at 1,000 years and “at a 95% level of confidence.” The Pahute Mesa Phase I flow model described in this report provides, through the flow fields derived from alternative HFMs and recharge models, one part of the data required to compute the contaminant boundary. Other components include the simplified source term model, which incorporates uncertainty and variability in the factors that control radionuclide release from an underground nuclear test (SNJV, 2004a), and the transport model with the concomitant parameter uncertainty as described in Shaw (2003). The uncertainty in all the above model components will be analyzed to produce the final contaminant boundary.

10.0 REFERENCES

ASTM, see American Society for Testing and Materials.

American Society for Testing and Materials. 1993a. *Standard Guide for Application of a Ground-Water Flow Model to a Site-Specific Problem*, ASTM D 5447-93. Philadelphia, PA.

American Society for Testing and Materials. 1993b. *Standard Guide for Comparing Ground-Water Flow Model Simulations to Site-Specific Information*, ASTM D 5490-93. Philadelphia, PA.

American Society for Testing and Materials. 1994a. *Standard Guide for Defining Boundary Conditions in Ground-Water Flow Modeling Designation*, ASTM D 5609-94. Philadelphia, PA.

American Society for Testing and Materials. 1994b. *Standard Guide for Defining Initial Conditions in Ground-Water Flow Modeling*, ASTM D 5610-94. Philadelphia, PA.

American Society for Testing and Materials. 1994c. *Standard Guide for Conducting a Sensitivity Analysis for a Ground-Water Flow Model Application*, ASTM D 5611-94. Philadelphia, PA.

American Society for Testing and Materials. 1996. *Standard Guide for Calibrating a Ground-Water Flow Model Application*, ASTM D 5981-96. Philadelphia, PA.

Anderson, M.P. 1979. "Using Models To Simulate the Movement of Contaminants Through Groundwater Systems." In *Critical Reviews in Environmental Control*, v. 9(2): 97-156. CRC Press.

Anderson, M.P., and W.W. Woessner. 1992. *Applied Groundwater Modeling*. San Diego, CA: Academic Press.

Ashby, S.F. 1996. *ParFlow Project*. Livermore, CA: Lawrence Livermore National Laboratory.

BN, see Bechtel Nevada.

Bechtel Nevada. 2002. *A Hydrostratigraphic Model and Alternatives for the Groundwater Flow and Contaminant Transport Model of Corrective Action Units 101 and 102: Central and Western Pahute Mesa, Nye County, Nevada*, DOE/NV/11718--706. Las Vegas, NV.

- Belcher, W.R., J.B. Blainey, F.A. D’Agnese, C.C. Faunt, M.C. Hill, R.J. Laczniak, G.M. O’Brien, C.J. Potter, H.M. Putnam, C.A. San Juan, and D.S. Sweetkind. 2004. *Death Valley Regional Model Ground-Water Flow System, Nevada and California - Hydrogeologic Framework and Transient Ground-Water Flow Model*, Scientific Investigations Report 2004-5205. U.S. Geological Survey.
- Blankennagel, R.K., and J.E. Weir, Jr. 1973. *Geohydrology of the Eastern Part of Pahute Mesa, Nevada Test Site, Nye County, Nevada*, Professional Paper 712-B. Denver, CO: U.S. Geological Survey.
- Bonnlander, B.V., and A.S. Weigend. 1994. “Selecting Input Variables Using Mutual Information and Nonparametric Density Estimation,” Proc., *International Symposium on Artificial Neural Networks (ISANN'94)*, 42-50. Tainan, Taiwan.
- Bredehoeft, J.D. 2005. “The Conceptualization Model Problem — Surprise.” In *Hydrogeology Journal*, v. 13(1): 37-46.
- Breiman, L., J.H. Friedman, R.A. Olshen, and C.J. Stone. 1984. *Classification and Regression Trees*. Monterey, CA: Wadsworth and Brooks/Cole.
- Butler, J.J., Jr. 1997. *The Design, Performance, and Analysis of Slug Tests*. Campus West, University of Kansas. CRC Press.
- CRWMS M&O, see Civilian Radioactive Waste Management System Management and Operating Contractor.
- Caine, J.S., J.P. Evans, and C.B. Forster. 1996. “Fault Zone Architecture and Permeability Structure.” In *Geology*, v. 24(11): 1025-1028.
- Carrera, J., and S.P. Neuman. 1986a. “Estimation of Aquifer Parameters Under Transient and Steady State Conditions: 1. Maximum Likelihood Method Incorporating Prior Information.” In *Water Resources Research* v. 22(2): 199-210.
- Carrera, J., and S.P. Neuman. 1986b. “Estimation of Aquifer Parameters Under Transient and Steady State Conditions: 3. Application to Synthetic and Field Data.” In *Water Resources Research*, v. 22(2): 228-242.
- Chapman, J.B., R.L. Hershey, and B.F. Lyles. 1995. *Groundwater Velocities at the Nevada Test Site: ¹⁴C Carbon-Based Estimates*, DOE/NV/11508-03 UC-703; Publication No. 45135. Las Vegas, NV: Desert Research Institute.
- Civilian Radioactive Waste Management System Management and Operating Contractor. 1997. *ISM2.0: A 3D Geologic Framework and Integrated Site Model of Yucca Mountain*, B000000000-0717-5700-004, Rev. 00. Las Vegas, NV.

- Civilian Radioactive Waste Management System Management and Operating Contractor. 2000. *Integrated Site Model Process Report*, TDR-NBS-GS-000002, REV 00, ICN 01. Las Vegas, NV: TRW Environmental Safety Systems, Inc.
- Cook, P., and J.K. Bohlke. 2000. "Determining Timescales for Groundwater Flow and Solute Transport." In *Environmental Tracers in Subsurface Hydrology*, pp.1-30. Boston, MA: Kluwer.
- Cover, T.M., and J.A. Thomas. 1991. *Elements of Information Theory*. New York, NY: John Wiley & Sons, Inc.
- DOE/NV, see U.S. Department of Energy, Nevada Operations Office.
- DOE/ORD, see U.S. Department of Energy, Office of Civilian Radioactive Waste Management, Office of Repository Development.
- D'Agnesse, F.A., C.C. Faunt, A.K. Turner, and M.C. Hill. 1997. *Hydrogeologic Evaluation and Numerical Simulation of the Death Valley Regional Ground-water Flow System, Nevada and California: Water-Resources Investigations Report 96-4300*, p. 124. Denver, CO: U.S. Geological Survey.
- Dash, Z.V. 2000. *Validation Test Report (VTR) for the FEHM Application Version 2.10, Yucca Mountain Project Identification Numbers SAN: LANL-1999-046; STN: 10086-2.10-00*. Los Alamos, NM: Los Alamos National Laboratory.
- Dash, Z.V. 2001. *Validation Test Report (VTR) for the FEHM Application Version 2.12, Yucca Mountain Project Identification Numbers SAN: LANL-2001-133; STN: 10086-2.12-00*. Los Alamos, NM: Los Alamos National Laboratory.
- Dash, Z.V., B.A. Robinson, and G.A. Zyvoloski. 1997. *Software Requirements, Design, and Verification and Validation for the FEHM Application - A Finite-Element Heat- and Mass-Transfer Code*, LA-13305-MS. Los Alamos, NM: Los Alamos National Laboratory.
- Drellack, S.L., and L.B. Prothro. 1997. *Descriptive Narrative for the Hydrogeologic Model of Western and Central Pahute Mesa Corrective Action Units*. Las Vegas, NV: Bechtel Nevada.
- Duffield, G.M., J.J. Benegar, and D.S. Ward. 1996. *MODFLOWT, A Modular Three-Dimensional Groundwater Flow and Transport Model, User's Manual, Version 1.1*. Sterling, VA: HSI GeoTrans, Inc.
- Dynamic Graphics, Inc. 2002. *EarthVision 5.1: Software for 3-D Modeling and Visualization*. Alameda, CA.
- FFACO, see *Federal Facility Agreement and Consent Order*.

- Faunt, C.C. 1997. *Effect of Faulting on Ground-Water Movement in the Death Valley Region, Nevada and California*, Water-Resources Investigations Report 95-4132. Denver, CO: U.S. Geological Survey.
- Faunt, C.C., F.A. D’Agnese, and G.M. O’Brien 2004. *Death Valley Regional Ground-Water Flow System, Nevada and California--Hydrogeologic Framework and Transient Ground-Water Flow Model*, Scientific Investigations Report 2004-5205, Chapter D, Hydrology, pp. 137-163. U.S. Geological Survey.
- Federal Facility Agreement and Consent Order*. 1996, as amended. Agreed to by the State of Nevada, the U.S. Department of Energy, and the U.S. Department of Defense. Appendix VI, which contains the Underground Test Area strategy, was last amended December 7, 2000, Revision No. 1.
- Fenelon, J.M. 2000. *Quality Assurance and Analysis of Water Levels in Wells on Pahute Mesa and Vicinity, Nevada Test Site, Nye County, Nevada*, Water-Resources Investigations Report 00-4014. Carson City, NV: U.S. Geological Survey.
- Ferguson, J.F., A.H. Cogbill, and R.G. Warren. 1994. “A Geophysical- Geological Transect of the Silent Canyon Caldera Complex, Pahute Mesa, Nevada.” In *Ground Water*, v. 99(B3): 4323-4339. Columbus, OH: Groundwater Publishing Co.
- Freyberg, D.L. 1988. “An Exercise in Ground-Water Model Calibration and Prediction.” In *Ground Water*, v. 26(N3): 350-360.
- Fridrich, C.J., S.A. Minor, and E.A. Mankinen. 1999a. *Geologic Evaluation of the Oasis Valley Basin, Nye County, Nevada*. U.S. Geological Survey Open-File Report 99-533-A.
- Fridrich, C.J., S.A. Minor, P.L. Ryder, and J.L. Slate. 1999b. *Geologic Map of the Oasis Valley Basin and Vicinity Nye County, Nevada*. U.S. Geological Survey Open-File Report 99-533-B, scale 1:62,500.
- GeoTrans, see HSI GeoTrans.
- Gable, C., and T. Cherry. 2001. *Technical Note on Interpolation of MODFLOW Flux onto a Piecewise Linear Surface*. Los Alamos, NM: Los Alamos National Laboratory.
- Gelhar, L. 1986. “Stochastic Subsurface Hydrology From Theory to Applications.” In *Water Resources Research*, v. 22(9): 135S-145S. Washington, DC: American Geophysical Union.
- Gentleman, R., and R. Ihaka. 2005. *An Integrated Suite of Software Facilities for Data Manipulation, Calculation and Graphical Display*. Auckland, New Zealand: University of Auckland.

- George, D.C. 1997. *Unstructured 3D Grid Toolbox for Modeling and Simulation*, LA-UR-97-3052. Los Alamos, NM: Los Alamos National Laboratory.
- Gillespie, D. 2003. *Temperature Data Evaluation*, DOE/NV/13609-22. Las Vegas, NV: Desert Research Institute.
- Granger, C.W.J., and J. Lin. 1994. "Using Mutual Information To Identify Lags in Nonlinear Models." In *Journal of Time Series Analysis*, v. 15: 371-384.
- Grauch, V.J.S., D.A. Sawyer, C.J. Fridrich, and M.R. Hudson. 1997. *Geophysical Interpretations West of and Within the Northwestern Part of the Nevada Test Site*. U.S. Geological Open-File Report 97-476. Denver, CO.
- Gupta, S. 1996. *CFEST, Flow and Solute Transport, Draft User's Manual*. Irvine, CA: Consultant for Environmental System Technologies (CFEST).
- Harrar, W.G. T.O. Sonnenborg, H.J. Henriksen. 2003. "Capture Zone, Travel Time, and Solute-Transport Predictions Using Inverse Modeling and Different Geological Models." In *Hydrogeology Journal*, v. 11: 536-548.
- Hevesi, J.A., A.L. Flint, and L.E. Flint. 2003. *Simulation of Net Infiltration and Potential Recharge Using a Distributed Parameter Watershed Model for the Death Valley Region, Nevada and California*, Water-Resources Investigations Report 03-4090. Sacramento, CA: U.S. Geological Survey.
- Hill, M.C. 1998. *Methods and Guidelines for Effective Model Calibration*, Water-Resources Investigations Report 98-4005. Denver, CO: U.S. Geological Survey.
- HSI GeoTrans. 1990. *Data Input For Swift III, The Sandia Waste-Isolation Flow and Transport Model for Fractured Media, Release 2.32*. Based on original report by: Reeves, M., D.S. Ward, N.D. Johns, and R.M. Cranwell. Originally prepared: December 1985. Herndon, VA: Modifications to Report NUREG/CR-3162.
- HSI GeoTrans. 1998. *Theory and Implementation for SWIFT-98: The Sandia Waste-Isolation Flow and Transport Model for Fractured Media*. Sterling, VA: HSI GeoTrans.
- Iman, R.L., and W.J. Conover. 1979. "The Use of Rank Transform in Regression." In *Technometrics*, v. 21(4): 499-509.
- Iman, R.L., J.M. Davenport, and D.K. Ziegler. 1980. *Latin Hypercube Sampling Program User's Guide*, SAND79-1473. Albuquerque, NM: Sandia National Laboratories.
- Intercomp. 1976. *A Model for Calculating Effects of Liquid Waste Disposal in Deep Saline Aquifer*, Water-Resources Investigations Report 76061. Prepared for the U.S. Geological Survey: Reston, VA.

IT, see IT Corporation.

IT Corporation. 1996a. *Groundwater Recharge and Discharge Data Documentation Package (Phase I Data Analysis Documentation, Volume III)*, ITLV/10972-181. Las Vegas, NV.

IT Corporation. 1996b. *Hydrologic Parameter Data Documentation Package (Phase I Data Analysis Documentation, Volume IV)*, ITLV/10972-181. Las Vegas, NV.

IT Corporation. 1996c. *Potentiometric Data Documentation Package (Phase I Data Analysis Documentation, Volume II)*, ITLV/10972-181. Las Vegas, NV.

IT Corporation. 1996d. *Regional Geologic Model Data Documentation Package (Phase I Data Analysis Documentation, Volume I)*, ITLV/10972-181. Las Vegas, NV.

IT Corporation. 1996e. *Transport Parameter and Source Term Data Documentation Package (Phase I Data Analysis Documentation, Volume V)*, ITLV/10972-181. Las Vegas, NV.

IT Corporation. 1996f. *Tritium Transport Model Documentation Package (Phase I Data Analysis Documentation, Volume VII)*, ITLV/10972-181. Las Vegas, NV.

IT Corporation. 1997a. *Groundwater Flow Model Documentation Package (Phase I Data Analysis Documentation, Volume VI)*, ITLV/10972-181. Las Vegas, NV.

IT Corporation. 1997b. *Risk Assessment Documentation Package (Phase I Data Analysis Documentation, Volume VIII)*, ITLV/10972-181. Las Vegas, NV.

IT Corporation. 1998a. *Report and Analysis of the BULLION Forced-Gradient Experiment*, ITLV/13052-042, DOE/NV-13-52. Las Vegas, NV.

IT Corporation. 1998b. *Value of Information Analysis for Corrective Action Units Nos. 101 and 102: Central and Western Pahute Mesa, Nevada Test Site, Nevada*, ITLV/13052-041. Las Vegas, NV.

IT Corporation. 1998c. *Western Pahute Mesa – Oasis Valley Hydrogeologic Investigation Wells Drilling and Completion Criteria*, Rev. 0, ITLV/13052-049, p. 439. Las Vegas, NV.

IT Corporation. 1999. *Underground Test Area Project Corrective Action Unit 98: Frenchman Flat, Vol. II, Groundwater Data Documentation Package*, Rev. 0, DOE/NV/13052-044-V2. Las Vegas, NV.

IT Corporation. 2001. *Underground Test Area Fracture Analysis Report: Analysis of Fractures in Volcanic Rocks of Western Pahute Mesa-Oasis Valley*, ITLV/13052-150. Las Vegas, NV.

Katyal, A.K. 1995. *CSMoS Online Model Information for BIOF&T-3D*. U.S. Environmental Protection – Ada Oklahoma Laboratory. Blacksburg, VA: Draper Aden Environmental Modeling, Inc.

- Kersting, A.B., D.W. Efurud, D.L. Finnegan, D.J. Rokop, D.K. Smith, and J.L. Thompson. 1999. "Migration of Plutonium in Groundwater at the Nevada Test Site." In *Nature*, v. 397: 56-59.
- Kipp, K.L., Jr. 1986. *HST3D: A Computer Code for Simulation of Heat and Solute Transport in Three-Dimensional Ground-water Flow Systems*, Water-Resources Investigations Report 86-4095. Denver, CO: U.S. Geological Survey.
- Kwicklis, E.M., T.P. Rose, and F.C. Benedict. 2005. *Evaluation of Groundwater Flow in the Pahute Mesa – Oasis Valley Flow System Using Groundwater Chemical and Isotopic Data*, LA-UR 05-4344. Los Alamos, NM: Los Alamos National Laboratory.
- Laczniak, R.J., J.C. Cole, D.A. Sawyer, and D.A. Trudeau. 1996. *Summary of Hydrogeologic Controls on Ground-Water Flow at the Nevada Test Site, Nye County, Nevada*, Water-Resources Investigations Report 96-4109. Denver, CO: U.S. Geological Survey.
- Laczniak, R.J., J.L. Smith, P.E. Elliott, G.A. DeMeo, M.A. Chatigny, and G. Roemer. 2001. *Ground-Water Discharge Determined from Estimates of Evapotranspiration, Death Valley Regional Flow System, Nevada and California*, Water-Resources Investigations Report 01-4195. Denver, CO: U.S. Geological Survey.
- Maxey, G.B., and T.E. Eakin. 1949. "Groundwater in White River Valley, White Pine, Nye and Lincoln Counties, Nevada." In *Water Resources*, Bulletin No. 8. Carson City, NV: State of Nevada, Office of the State Engineer.
- McDonald, M.G., and A.W. Harbaugh. 1988. *Techniques of Water-Resources Investigations of the United States Geological Survey, A Modular Three-Dimensional Finite-Difference Ground-Water Flow Model*, Book 6, Chapter A1. Washington, DC: U.S. Geological Survey.
- McKay, M.D., W.J. Conover, and R.J. Beckman. 1979. "A Comparison of Three Methods for Selecting Values of Input Variables in the Analysis of Output from a Computer Code." In *Technometrics*, v. 21(3): 239-245.
- McKee, E.H., T.G. Hildenbrand, M.L. Anderson, P.D. Rowley, and D.A. Sawyer. 1999. *The Silent Canyon Caldera Complex: Three Dimensional Model Based on Drill-Hole Stratigraphy and Gravity Inversion*, Open-File Report 99-555, p. 38. Las Vegas, NV: U.S. Geological Survey.
- McKee, E.H., G.A. Phelps, and E.A. Mankinen. 2001. *The Silent Canyon Caldera: Three-Dimensional Model as Part of a Pahute Mesa-Oasis Valley, Nevada Hydrogeologic Model*, Open-File Report 01-297. Las Vegas, NV: U.S. Geological Survey.
- Mishra, S., and R.G. Knowlton. 2003. "Testing for Input-Output Dependence in Performance Assessment Models," Proc., *Tenth International High-Level Radioactive Waste Management Conference*, March 30 - April 2. Las Vegas, NV.

- Mishra, S., N.E. Deeds, and B.S. RamaRao. 2003. "Application of Classification Trees in the Sensitivity Analysis of Probabilistic Model Results." In *Reliability Engineering & System Safety*, v. 73: 123-129.
- Moddemeijer, R. 1989. "On the Estimation of Entropy and Mutual Information of Continuous Distributions." In *Signal Processing*, v. 16(3): 233-248.
- NRC, see National Research Council.
- Naff, R.L. 1978. *A Continuum Approach to the Study and Determination of Field Longitudinal Dispersion Coefficients*, PhD Dissertation. Socorro, NM: New Mexico Institute of Mining and Technology.
- National Research Council. 1996. *Rock Fractures and Fluid Flow: Contemporary Understanding and Applications*. Washington, DC: National Academy Press.
- Neuman, S.P. 1990. "Universal Scaling of Hydraulic Conductivities and Dispersivities in Geologic Media." In *Water Resources Research*, v. 26 (8): 1749-1758. American Geophysical Union.
- Nishikawa, T. 1997. "Testing Alternative Conceptual Models of Seawater Intrusion in a Coastal Aquifer Using Computer Simulation, Southern California, USA." In *Hydrogeology Journal*, v. 5(3): 60-74.
- Nitao, J.L. 1998. *User's Manual for the USNT Module of the NUFT Code, Version 2.0*, UCRL-MA-130653. Livermore, CA: Lawrence Livermore National Laboratory.
- Noble, D.C., G.D. Bath, R.L. Christiansen, and P.P. Orkild. 1968. *Zonal Relations and Paleomagnetism of the Spearhead and Rocket Wash Members of the Thirsty Canyon Tuff, Southern Nevada*, Professional Paper 600C: C61-65. Denver, CO: U.S. Geological Survey.
- O'Hagan, M.D., and R.J. Lacznik. 1996. *Ground-Water Levels Beneath Eastern Pahute Mesa and Vicinity, Nevada Test Site, Nye County, Nevada*, Water-Resources Investigations Report 96-4042. Denver, CO: U.S. Geological Survey.
- Orkild, P.P., K.A. Sargent, and R.P. Snyder. 1969. *Geologic Map of Pahute Mesa, Nevada Test Site and Vicinity, Nye County, Nevada*, Map I-567, scale: 1: 48,000. Denver, CO: U.S. Geological Survey.
- Parkhurst, D.L., and C.A.J. Appelo. 1999. *User's Guide to PHREEQC (Version 2) — A Computer Program for Speciation, Batch-Reaction, One-Dimensional Transport, and Inverse Geochemical Calculations*, Water-Resources Investigations Report 99-4259, p. 312. U.S. Geological Survey.
- Pawloski, G.A., A.F.B. Tompson, and S. Carle, eds. 2001. *Evaluation of the Hydrologic Source Term from Underground Nuclear Tests on Pahute Mesa at the Nevada Test Site: The CHESHIRE Test*, UCRL-ID-147023. Livermore, CA: Lawrence Livermore National Laboratory.

- Plummer, L.N., E.C. Prestemon, and D.L. Parkurst. 1994. *An Interactive Code (NETPATH) for Modeling Net Geochemical Reactions Along a Flow Path*, Version 2.0, Water-Resources Investigations Report 94-4169. Denver, CO: U.S. Geological Survey.
- Poeter, E.P., and M.C. Hill. 1997. "Inverse Models: A Necessary Next Step in Ground-Water Modeling." In *Ground Water*, v. 35(N2): 250-260.
- Pollock, D.W. 1988. "Semianalytical Computation of Path Lines for Finite-Difference Models." In *Ground Water*, v. 26: 743-750.
- Press, W.H., S.A. Teukloksky, W.T. Vetterling, and B.P. Flannery. 1992. *Numerical Recipes in FORTRAN*, LBL-29400. Cambridge University Press: London.
- Prothro, L.B., and R.G. Warren. 2001. *Geology in the Vicinity of the TYBO and BENHAM Underground Nuclear Test, Pahute Mesa, Nevada Test Site*. Los Alamos National Laboratory and Bechtel Nevada Report DOE/NV11718--305.
- Pruess, K. 1991. *TOUGH2 - A General Purpose Numerical Simulator for Multiphase Fluid and Heat Flow*. Berkeley, CA: Lawrence Berkeley Laboratory.
- Reeves, M., D.S. Ward, N.D. Johns, and R.M. Cranwell. 1986. *Theory and Implementation for SWIFT II, The Sandia Waste-Isolation Flow and Transport Model for Fractured Media*, NUREG/CR3328. Albuquerque, NM: Sandia National Laboratories.
- Reiner, S.R., R.J. Laczniaik, G.A. DeMeo, J. LaRue Smith, P.E. Elliott, W.E. Nylund, and C.J. Fridrich. 2002. *Ground-Water Discharge Determined from Measurements of Evapotranspiration, Other Available Hydrologic Components, and Shallow Water-Level Changes, Oasis Valley, Nye County, Nevada*, Water-Resources Investigations Report 01-4239. Carson City, NV: U.S. Geological Survey.
- Robinson, B.A. 2004. *Particle Tracking Model and Abstraction of Transport Processes*, MDL-NBS-HS-000020, REV 01, BSC LLC. Las Vegas, NV.
- Russell, C.E., and T. Minor. 2002. *Reconnaissance Estimates of Recharge Based on an Elevation-Dependent Chloride Mass-Balance Approach*, DOE/NV/11508-37. Las Vegas, NV: Desert Research Institute.
- Shaw, see Shaw Environmental, Inc.
- SNJV, see Stoller-Navarro Joint Venture.
- Saltelli, A., K. Chan, and M. Scott. 2000. *Sensitivity Analysis*. New York, NY: John Wiley & Sons Inc.

- Sawyer, D.A., and K.A. Sargent. 1989. "Petrologic Evolution of Divergent Peralkaline Magmas from the Silent Canyon Caldera Complex, Southwestern Nevada Volcanic Field." In *American Geophysical Union, Journal of Geophysical Research*, v. 94(B5): 6021-6040.
- Scheibe, T.D. and Y.-J. Chien. 2003. "An Evaluation of Conditioning Data for Solute Transport Prediction." In *Groundwater*, v. 41(2): 128.
- Scientific Software Group. 1998. *Information relating to the MT3D96 and 3DFEMFAT Computer Codes*. Sandy, UT.
- Scott, R.B., T.J. Smales, R.E. Rush, and A.S. Van Denburgh. 1971. "Water for Nevada, Nevada's Water Resources." In *State of Nevada Department of Conservation and Natural Resource, Water for Nevada Report 3*. Carson City, NV: Nevada Division of Water Resources.
- Seaton, W.J., and T.J. Burbey. 2005. "Influence of Ancient Thrust Faults on the Hydrogeology of the Blue Ridge Province." In *Groundwater*, v. 43(3): 301-314.
- Shaw Environmental, Inc. 2003. *Contaminant Transport Parameters for the Groundwater Flow and Contaminant Transport Model of Corrective Action Units 101 and 102: Central and Western Pahute Mesa, Nye County, Nevada*, Rev. 0, Shaw/13052-201-CD. Las Vegas, NV.
- Slate, J.L., M.E. Berry, P.D. Rowley, C.J. Fridrich, K.S. Morgan, J.B. Workman, O.D. Young, G.L. Dixon, V.S. Williams, E.H. McKee, D.A. Ponce, T.G. Hildenbrand, W.C. Swadley, S.C. Lundstrom, E.B. Ekren, R.G. Warren, J.C. Cole, R.J. Fleck, M.A. Lanphere, D.A. Sawyer, S.A. Minor, D.J. Grunwald, R.J. Laczniak, C.M. Menges, J.C. Yount, and A.S. Jayko. 1999. *Digital Geologic Map of the Nevada Test Site and Vicinity, Nye, Lincoln, and Clark Counties, Nevada, and Inyo County, California*, Open-File Report 99-554-A. Denver, CO: U.S. Geological Survey.
- Stoller-Navarro Joint Venture. 2004a. *Hydrologic Data for the Groundwater Flow and Contaminant Transport Model of Corrective Action Units 101 and 102: Central and Western Pahute Mesa, Nye County, Nevada*, Rev. 0, S-N/99205-002; Shaw/13052-204. Las Vegas, NV.
- Stoller-Navarro Joint Venture. 2004b. *Modeling Approach/Strategy for Corrective Action Units 101 and 102, Central and Western Pahute Mesa, Nye County, Nevada*, S-N/99205-008. Las Vegas, NV.
- Stoller-Navarro Joint Venture. 2004c. *Unclassified Source Term and Radionuclide Data for the Groundwater Flow and Contaminant Transport Model of Corrective Action Units 101 and 102: Central and Western Pahute Mesa, Nye County, Nevada*, Rev. 0, S-N/99205--022. Las Vegas, NV.
- Thomas, J.M., F.C. Benedict, Jr., T.P. Rose, R.L. Hershey, J.B. Paces, Z.E. Peterman, I.M. Farnham, K.H. Johannesson, A.K. Singh, K.J. Stetzenbach, G.B. Hudson, J.M. Kenneally, G.F. Eaton, and D.K. Smith. 2002. *Geochemical and Isotopic Interpretations of Groundwater Flow in the Oasis*

Valley Flow System, Southern Nevada, DOE/NV/11508-56; Publication No. 45190. Las Vegas, NV: Desert Research Institute.

Tompson, A.F.B., C.J. Bruton, and G.A. Pawloski, eds. 1999. *Evaluation of the Hydrologic Source Term from Underground Nuclear Tests in Frenchman Flat at the Nevada Test Site: The CAMBRIC Test*, UCRL-ID-132300. Livermore, CA: Lawrence Livermore National Laboratory.

U.S. Department of Energy, Nevada Operations Office. 1996. *Recompletion Report and Summary of Well History for Well PM-3*, DOE/NV-437 UC700. Las Vegas, NV.

U.S. Department of Energy, Nevada Operations Office. 1997. *Regional Groundwater Flow and Tritium Transport Modeling and Risk Assessment of the Underground Test Area, Nevada Test Site, Nevada*, DOE/NV--477. Las Vegas, NV.

U.S. Department of Energy, Nevada Operations Office. 1999. *Corrective Action Investigation Plan for Corrective Action Units 101 and 102, Central and Western Pahute Mesa, Nevada Test Site, Nevada*, DOE/NV--516, Rev. 1. Las Vegas, NV.

U.S. Department of Energy, Nevada Operations Office. 2000. *United States Nuclear Tests, July 1945 through September 1992*, DOE/NV-209, Rev. 15. Las Vegas, NV.

U.S. Department of Energy, Office of Civilian Radioactive Waste Management, Office of Repository Development. 2004. *Site-Scale Saturated Zone Transport*, MDL-NBS-HS-000010, ICN 00, Rev. 1. Las Vegas, NV.

Vatnaskil Consulting Engineers. 1988. *AQUA3D Groundwater Flow and Transport Model*. Sudurlandsbraut 50, 108 Reykjavik, Iceland.

Watermark, see Watermark Numerical Computing and Waterloo Hydrogeologic.

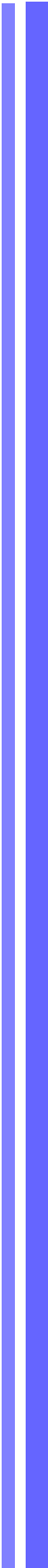
Ward, D.S., M. Reeves, and L.E. Duda. 1984. *Verification and Field Comparison of the Sandia Waste-Isolation Flow and Transport Model (SWIFT)*, NUREG/CR3316. Albuquerque, NM: Sandia National Laboratories.

Warren, R.G, D.A. Sawyer, F.M. Byers, and G.L. Cole. 2003. *A Petrographic, Geochemical, and Geophysical Database, and Stratigraphic Framework for the Southwestern Nevada Volcanic Field*, LA-UR-03-1503. Albuquerque, NM: Los Alamos National Laboratory.

Waterloo Hydrogeologic, Inc. 1998. *FRAC3DVS: Variably-Saturated Groundwater Flow and Transport in Discretely Fractured Porous Media*. Waterloo, Ontario, Canada.

Watermark Numerical Computing. 2004. *PEST Model-Independent Parameter Estimation Software*. Brisbane, Australia.

- Watrus, J. 2004. Personal communication to G. Ruskauff (SNJV) regarding Spot Springs, 24 March. Las Vegas, NV.
- Weiss, R., and L. Smith. 1993. "Parameter Estimation using Hydraulic Head and Environmental Tracer Data." Proc. of the Groundwater Modeling Conference, June 9-12, 1993. Golden, CO.
- Weiss, R., and L. Smith. 1997. "Efficient and Responsible Use of Prior Information in Inverse Methods." In *Groundwater*, v. 36(1): 151.
- Westinghouse Hanford Company. 1991. *PORMC: A Model for Monte Carlo Simulation of Fluid Flow, Heat, and Mass Transport in Variably Saturated Geologic Media*, WHC-EP-0445. Richland, WA.
- White, A.F. 1979. *Geochemistry of Ground Water Associated with Tuffaceous Rocks, Oasis Valley, Nevada*, Professional Paper 712-E. Denver, CO: U.S. Geological Survey.
- Winograd, I.J., and W. Thordarson. 1975. *Hydrogeologic and Hydrochemical Framework, South-Central Great Basin, Nevada-California, with Special Reference to the Nevada Test Site*, Professional Paper 712-C. Denver, CO: U.S. Geological Survey.
- Wolfsberg, A., L. Glascoe, G. Lu, A. Olson, P. Lichtner, M. McGraw, T. Cherry, and G. Roemer. 2002. *TYBO/BENHAM: Model Analysis of Groundwater Flow and Radionuclide Migration from Underground Nuclear Tests in Southwestern Pahute Mesa, Nevada*, LA-13977. Los Alamos, NM: Los Alamos National Laboratory.
- Zyvoloski, G.A., B.A. Robinson, Z.V. Dash, and L.L. Trease. 1996. *User's Manual for the FEHM Application*, LA-UR--94-3788, Rev. 1. Los Alamos, NM: Los Alamos National Laboratory.
- Zyvoloski, G.A., B.A. Robinson, Z.V. Dash, and L.L. Trease. 1997a. *Summary of Models and Methods for the FEHM Application - A Finite-Element Heat- and Mass-Transfer Code*, LA-13307-MS. Los Alamos, NM: Los Alamos National Laboratory.
- Zyvoloski, G.A., B.A. Robinson, Z.V. Dash, and L.L. Trease. 1997b. *User's Manual for the FEHM Application - A Finite-Element Heat- and Mass-Transfer Code*, LA-13306-M. Los Alamos, NM: Los Alamos National Laboratory.
- Zyvoloski, G.A., E. Kwicklis, A.A. Eddebarh, B. Arnold, C. Faunt, and B.A. Robinson. 2003. "The Site-Scale Saturated Zone Flow Model for Yucca Mountain: Calibration of Different Conceptual Models and Their Impact on Flow Paths." In *Journal of Contaminant Hydrology*, v. 62-63: 731-750.



Appendix A

Evaluation of Flow and Transport Codes for Application to the Western Pahute Mesa Corrective Action Unit

This appendix contains the letter report documenting the evaluation of flow and transport codes for application to the Western Pahute Mesa Corrective Action Unit. This letter report was completed on September 2, 1999, and provided the basis for a presentation to the Technical Working Group Modeling Subcommittee on September 23, 1999.

A.1.0 INTRODUCTION

The code evaluation task consists of the selection and evaluation of three numerical codes in support of the Western Pahute Mesa Corrective Action Unit (CAU) modeling effort. The subtasks consist of identification of code attributes consistent with the key physical and chemical processes that must be simulated by the CAU scale model, identification of candidate codes, selection of three codes from the candidate codes for testing, development of a test problem, development of testing criteria, and evaluation against determined criteria of the performance of candidate codes in simulating the test problem. A quantitative evaluation of flow and transport on Western Pahute Mesa was not within the scope of work of this task. The test problem was simulated without calibration in some cases using extreme values of properties and hydrologic source terms in order to test the capabilities of the codes. With this in mind, it is important to note that the results of the test problem simulations should not in any way be interpreted as accurately representing the magnitudes of flow and transport processes occurring on Western Pahute Mesa.

A.2.0 CODE ATTRIBUTES

A number of attributes or capabilities of the CAU model were defined to satisfy the modeling objectives. The first objective requires the CAU model to have the ability to represent the important physical and chemical features of the CAU groundwater flow system. The features include faulting, stratigraphy, sources and sinks of water, the distribution of contaminants and their rates of introduction into the groundwater flow system, and other physical or chemical features unique to the CAU. The second objective requires the CAU model to simulate the movement of a variety of contaminants for which their distribution and abundance serve to define the contaminant boundary. The third objective requires flexibility in the CAU model to allow grid changes, placement of additional wells, and boundary condition variations. The required code attributes that were defined consistently with the three modeling objectives were categorized under “general,” “flow model,” and “transport model.” Each of these attributes will be described and assessed with respect to importance for the CAU modeling. In addition, six non-essential but desirable attributes were identified. These include: finite-element formulation, steady-state capability, double-porosity/double-permeability formulation, the ability to simulate the transport of multiple solutes and daughter products, and established pre- and post-processors.

A.2.1 General Attributes

Fully Three-Dimensional

The groundwater flow system is controlled by the distribution of geologic units as well as the location of sources and sinks of water. Additionally, transport properties including source location and strength, porosity, and diffusion may vary in space. The three-dimensional (3-D) nature of the groundwater flow system requires that the CAU model will need to be 3-D to adequately simulate migration of the potential contaminants within the CAU-model area.

Large Numbers of Nodes Capability

For a given formulation, the greater the number of nodes in the CAU model, the greater the detail that can be included. Given the anticipated large geographic area of the Pahute Mesa CAU model, the ability of the CAU model to simulate many nodes will control the amount of detail that can be included. In general, each of the selected codes will only be limited by the capacity of the hardware, not by the software used.

Multiple Boundary Condition Options

Options for specified pressure and specified flux boundary conditions for fluids, as well as specified temperature or specified heat flow, may be required in implementing the CAU model.

Transient Capability

The initial flow simulations for the CAU model will be steady-state with possible transient runs to follow. The contaminant transport simulations will all be performed under transient conditions.

Efficient Solver

To simulate in sufficient detail, the CAU model will require a large number of nodes as mentioned above. To make a large model practical, the codes must run efficiently. Generally, a code has a selection of solvers available. The solvers must be efficient enough to allow for more than one run per day. A code that requires more than six hours per simulation would be eliminated. A six-hour run time allows two runs per day on a single computer.

Acceptable Numerical Accuracy

The numerical solution of the transport equation is typically more difficult than the solution of the flow equation. This attribute requires the results of the code for a given test problem to have been checked against analytical solutions and against the results of other numerical codes for the same problem. Documentation of this quality assurance (QA) checking must be available.

Minimal Numerical Dispersion

Under certain circumstances, the error in the numerical approximation of a value can become as large as the value being approximated. When this occurs, the numerical solution combines an exclusively

numerical dispersion with the real hydrodynamic dispersion producing an overestimate of the actual dispersion. Solution techniques that minimize numerical dispersion are required.

Acceptable Verification and Validation

The degree of computer code verification and validation varies widely depending on the code being considered. The extent to which this process has been documented for a particular code varies even more. Thoroughly documented testing is required to ensure that the code satisfies requirements specified for its options and features.

Access to Source Code

Computer codes are initially written by humans in a high-level language such as FORTRAN and then translated into machine language for execution on the computer. The high-level version of the code is called the “source code,” and can be read and modified by humans. The machine-language version is called the “executable code,” can be deciphered only by the computer. Many distributors of computer codes provide only the executable version of the code to the user. During the course of the development or application of the CAU model, it may be necessary to examine or modify the step-by-step procedure implemented in the computer code. To accomplish this, access to the source code will be required.

A.2.2 Groundwater Flow Model Attributes

Saturated Groundwater Flow

The codes must be able to simulate saturated groundwater flow.

Heterogeneous and Anisotropic Hydraulic Conductivity

Aquifer heterogeneity reflects the natural variability in the subsurface. The CAU model must be capable of simulating flow through aquifers in which the hydraulic conductivity may vary from location to location. Anisotropy is a directional dependence of the hydraulic conductivity. In fractured aquifers, it is common for hydraulic conductivity to be larger in a direction parallel to fracturing and smaller perpendicular to fracturing.

Point and Distributed Sources and Sinks of Water

Recharge may occur over a large spatial area due to precipitation or may be concentrated into washes or craters. Discharge may occur at wells or individual springs or may occur over larger areas such as playas. The CAU model should have the capability to simulate these various cases.

Temperature Dependence

The flow of groundwater may be influenced by water temperature variations. Warm water is more buoyant than colder water and tends to rise. Additionally, warm water is less viscous and tends to move more easily than cold water. These processes may be important in some portions of the CAU where naturally occurring sources of heat have caused elevated groundwater temperatures. An additional source of warm water may be the underground test cavities. It may be important to account for these temperature effects in the simulations.

Simulate Complex Geology

The geology of Pahute Mesa is complex. It consists of multiple stratigraphic units, some of which are truncated by faults and other structural features. Even within units, changes in facies result in spatial variations in material properties. The flow of groundwater (amount and direction) is governed, in large part, by the distribution of geologic units. The code must be able to include important features of the geology such as lateral and vertical changes in material properties. Much of this attribute is similar to earlier general attributes related to number of grid nodes and simulation speed. The greater the number of nodes, the more detail that can be incorporated into the CAU model.

A.2.3 Transport Model Attributes

Advection, Dispersion, Sorption, and Matrix Diffusion

It is expected that advection (via the groundwater flux) and matrix diffusion will be the primary factors influencing tritium transport. It is expected that sorption will also be important for reactive contaminants, but this may not be the dominant contributor to the location of contaminant boundary. Dispersion is included because it may be important at smaller scales.

Radioactive Decay

Most, but not all, of the potential contaminants of interest are radionuclides. The activity per volume of radionuclides decreases via the process of radioactive decay.

A.2.4 Desirable Attributes

These are attributes of the computer codes that were considered valuable but not essential to satisfying the CAU-modeling objectives.

Finite Element Formulation

A finite element formulation allows much more flexibility in representing the geology being modeled. Grids can be developed to represent complex structures such as faults, pinch outs and layer truncations. In addition, grid refinement allows the grid to be modified to provide more resolution in the area of interest.

Steady-State Capability

Some of the codes do not include a steady flow option, but rather reach steady-state by leaving parameters fixed in time and performing transient simulations over large periods of time until steady-state is reached. This approach is adequate, but somewhat slower than if a true steady-state option were available.

Double-Porosity/Double-permeability Formulation

The double-porosity/double-permeability method is similar to the double-porosity method in that it allows for communication between fractures and matrix material. The term dual porosity/dual permeability is often used in the literature. In this report, dual is used interchangeably with double depending on the usage in the model documentation. This feature allows for the modeling of matrix diffusion. The double-porosity/double-permeability method differs in that it allows matrix cells that communicate with fractures to also communicate with other matrix cells. While this method provides a more realistic simulation, its use is more important for unsaturated flow problems.

Multiple Solutes

Many codes are designed to provide a simulation of the migration of a single solute in a given run. Using a code with the ability to model transport for multiple solutes in a single run may be more efficient.

Daughter Products

A radionuclide may decay into another radionuclide (called a daughter product) or into a stable isotope. More accurate estimates of dose can be obtained if the code is capable of simulating the ingrowth and transport of a radionuclide and daughter product(s).

Established Pre- and Post-Processors

The task of creating the input datasets for any model is simplified by having pre-processors take data and put it into a form that is required by the model. Post-processors take model output and typically create graphic images of some simulated parameter such as water level or solute concentration. Pre- and post-processors generally speed up the modeling task.

A.3.0 CODE IDENTIFICATION AND PRELIMINARY SELECTION

The following list includes the codes initially screened for the Pahute Mesa CAUs:

- AQUA3D (Vatnaskil Consulting Engineers, 1988)
- BIOF&T-3D (Katyal, 1995)
- CFEST (Gupta, 1996)
- FEHM (Zyvoloski, et al., 1997a)
- FRAC3DVS (Waterloo Hydrogeologic Inc., 1998)
- HST3D (Kipp, 1986)
- MODFLOWT (Duffield, et al., 1996)
- MT3D96 (Scientific Software Group, 1998)
- NUFT (Nitao, 1998)
- PARFLOW (Ashby, et al., 1996)
- PORMC (Westinghouse Hanford Co., 1991)
- SWIFT-1998 (HSI-GeoTrans, 1998)
- TOUGH2 (Pruess, 1991)
- 3DFEMFAT (Scientific Software Group, 1998)

An initial comparison of the codes was performed with respect to the attributes. The results of the comparison are presented in [Table A.11-1](#) where the required code attributes have been grouped into the categories of general, flow model, and transport model. Comparisons of attributes considered desirable, but not required, are also shown.

Of this list, ten codes were eliminated from further consideration. Seven codes: CFEST, HST3D, MT3D96, PARFLOW, PORMC, TOUGH2, AND 3DFEMFAT were eliminated because they do not have the ability to simulate matrix diffusion explicitly. BIOF&T-3D and AQUA3D were eliminated because access to the source codes was not available. NUFT was eliminated because current documentation (Nitao, 1998) indicated that hydrodynamic dispersion was not implemented in the code and in addition, the source code was not accessible.

Of the remaining four codes, only FEHM and SWIFT-98 have all of the required attributes. FRAC3DVS and MODFLOWT lacked only the ability to simulate thermal effects. FRAC3DVS was

ranked above MODFLOWT and retained for testing because its finite element formulation would allow a more accurate representation of the complex geology. Therefore, the three codes that were retained for further evaluation are FEHM, FRAC3DVS, and SWIFT-98.

A.4.0 DESCRIPTION OF THE CANDIDATE CODES

Features of the three codes identified as possible candidates for use in the Pahute Mesa CAU model are described below.

FRAC3DVS

FRAC3DVS (Waterloo Hydrologic, Inc., 1998) is a 3-D, finite element code for simulating steady-state or transient, variably-saturated groundwater flow, and advective-dispersive solute transport in porous or discretely-fractured porous media. The code was developed by E.A. Sudicky, at the Waterloo Centre for Groundwater Research, and R. Thierren at Laval University. Specific capabilities of this code include:

- 3-D
- flow of water
- multi-species transport of either straight or branching decay chains
- sorption according to a linear Freundlich isotherm
- control-volume finite element, Galerkin finite element, or finite difference formulation
- saturated and unsaturated media
- conjugate-gradient-like solver
- dual porosity and discrete fracture capabilities
- irregular, layered grids composed of blocks or prisms

SWIFT-98

The SWIFT-98 (Sandia Waste Isolation Flow and Transport) computer code (Reeves et al., 1986; Ward et al., 1984; Ward and Benegar, 1998) is a 3-D ground water flow and transport code designed to simulate the advective-dispersive transport of solutes, including radionuclides, in groundwater. The code is based on a block-centered finite-difference scheme. SWIFT evolved from the USGS SWIP (Survey Waste Injection Program). The current version, SWIFT-98 (Ward and Benegar, 1998), contains the following capabilities:

- 3-D
- advective-dispersive solute transport

- first-order decay and adsorption/desorption based on linear or nonlinear Freundlich isotherms
- inclusion of up to three daughter products for radionuclide transport simulations
- dual-porosity/dual-permeability
- brine and heat transport in porous or fractured media
- planar or spherical matrix block geometries
- transient and steady-state flow options
- centered or backwards differencing schemes in both time and space
- direct solver and two-line successive over-relaxation scheme

FEHM

The FEHM code (Zyvoloski et al., 1997a), developed by Los Alamos National Laboratory (LANL), simulates 3-D, time-dependent, multiphase, multicomponent, nonisothermal, reactive groundwater flow through porous and fractured media. FEHM's finite element formulation provides an accurate representation of complex 3-D geologic media and structures and their effects on subsurface flow and transport. Specific capabilities include:

- 3-D
- flow of gas, water, oil, and heat
- flow of air, water, and heat
- multiple chemically reactive and sorbing tracers
- colloid transport
- finite element/finite volume formulation
- coupled stress module
- saturated and unsaturated media
- preconditioned conjugate gradient solution of coupled nonlinear equations
- double porosity and double porosity/double-permeability capabilities
- complex geometries with unstructured grids

A number of documents supporting the FEHM code are readily available from LANL.

Documentation includes a description of the mathematical models and numerical methods used by FEHM (Zyvoloski, et al., 1997b), the user's manual (Zyvoloski, et al., 1997a), documentation of the functional and performance requirements for FEHM, description of the FEHM software, the verification and validation plan, and description of the verification and validation activities (Dash et al., 1997).

A.5.0 TESTING CRITERIA

The criteria used to assess the codes range from a somewhat subjective assessment of ease of use to more quantifiable assessments such as the run time for a sample problem. The testing criteria are as follows:

Portability

The CAU model may be sent to independent reviewers as well as the State of Nevada. Each of these stakeholders may want to run the code themselves. This requires that the code, when complete, should require minimal special equipment or software in order to make it usable. Additionally, the CAU model will likely need to be run on a classified computer at the DOE Nevada Support Facility or another secure location to produce a final estimate of the contaminant boundary (results based on classified data will be reported in a classified report). The code and associated pre- and post-processors must be portable to the selected secure location to allow for efficient classified simulations.

QA Evaluation

The chosen code must have been appropriately verified to ensure the output is accurate. The QA evaluation refers to the level of documentation and testing for a code. The ability of the code to simulate the processes of interest is a function of the formulation of the equations and the quality of the programming. A code meets the QA requirements if its results have been verified against those of other codes as well as compared with analytical solutions. These comparisons must be documented before a code will be used for the Pahute Mesa model.

Ease of Use

The ease of use is a subjective judgment that assesses the modeler's degree of difficulty in getting the model running. This is, by necessity, a value judgment of the modeler and reflects the modeler's experience and background. A great deal of energy will be spent calibrating the CAU model and

setting up sensitivity and uncertainty analyses. A code that is difficult to use makes the job of calibration more difficult and reduces the code's portability. Ease of use includes factors such as the structure of the input datasets used in the model and the flexibility of pre-and post-processors.

Ability To Represent the CAU Hydrogeology

The primary geologic features that control flow need to be represented in the CAU model. These features include the hydrostratigraphy, physical boundaries, and structural features such as faults. In addition, the ability to model physical processes of concern (advection, dispersion, matrix diffusion, adsorption, and radioactive decay) is also important. The criteria also include an assessment of the ability of the model to include sufficient detail and stay within the memory limitations of the computer platform chosen for simulation.

Speed of Simulation

The time required for a solution is also of importance to the evaluation of the codes. The faster the code, the shorter the time to complete each model run. As calibration normally requires many (often greater than 100) model runs, the simulation time becomes a problem if it is too long. For the purposes of the CAU model, simulation times less than six hours for a steady-state flow simulation are acceptable. This length of simulation time will allow for two or three runs per day, which provides sufficient time to perform the calibration assuming up to 200 runs to calibrate.

A.6.0 TEST PROBLEM

A test problem was created to evaluate the candidate codes. The features of the test problem were chosen to mimic the conditions expected in the Pahute Mesa model area. By doing so, the effort to set up and run the problem could be evaluated as well as the assessment of the run times of the model. The features to be included in the test problem are: complex caldera geology such as lithologic and structural features, temperature-dependent flow, radionuclide migration from a cavity, and matrix diffusion.

The test problem was designed to mimic the expected level of complexity anticipated for Pahute Mesa. The Pahute Mesa hydrogeologic model developed by Bechtel Nevada (Drellack and Prothro, 1997) provided the definition and distribution of hydrostratigraphic units (HSU) for the test problem. The Pahute Mesa hydrogeologic model consists of structure contour maps of the top of hydrostratigraphic units in the Pahute Mesa area mapped at a resolution of 300 meters (m). A portion of the Pahute Mesa hydrogeologic model, approximately 21 kilometers (km) by 19.5 km by 5,500 m in depth, and rotated 5 degrees to the east was selected for the comparison. The locations of the test problem boundaries are shown in [Figure A.11-1](#). The 3-D hydrogeologic model is shown in [Figure A.11-2](#) as viewed from the southwest corner of the test problem area. The complexity of the hydrostratigraphic layering and occurrence of non-vertical faults is illustrated in a cross section of the model shown in [Figure A.11-3](#).

The hydrogeologic model for the test problem included all the hydrostratigraphic layers in the Pahute Mesa hydrogeologic model as well as many of the faults. When using finite-element codes, the grid flexibility is used to attempt to reproduce the stratigraphic contacts and fault contacts.

Finite-difference codes do not offer this flexibility; several identical horizontal and uniform grids must be stacked vertically to represent the model layers. Because of this limitation, faults must be represented as vertical. Thus, to use the finite-difference grid in the test problem, the faults will be approximated as vertical.

Each of the HSUs were assigned a hydraulic conductivity, porosity, and fracture volume fraction consistent with current best estimates of these properties.

Boundary conditions for the test problem were obtained from the MODFLOW regional model. The process used was to average the properties of the Pahute Mesa hydrogeologic model to the same resolution as the regional model. The hydrostratigraphic units from the Pahute Mesa hydrogeologic model were then added to the regional model. A visualization application, earthVision (eV), was used to examine the correspondence between the CAU scale model and the regional model. All layers were checked for inversions of layers, and that a constant thickness of at least 1 m vertically was maintained in the hydrogeologic model layering. Using this modified regional hydrogeologic model, the MODFLOW regional flow model was run, without re-calibration, to obtain the heads along the boundaries of the test problem.

Two nuclear tests were chosen for consideration as sources in the test problem, SERENA (U20an) and SCOTCH (U19as). The locations of these tests are shown in [Figure A.11-1](#). SERENA was chosen because of its location on a fault and SCOTCH was chosen because of the depth of the working point and the absence of faults in the immediate vicinity in the Pahute Mesa hydrogeologic model. While SCOTCH is in fact adjacent to the Scotch fault (Warren and LaDelfe, 1991), this fault is not currently included in the Pahute Mesa hydrogeologic model. Since the location of SCOTCH is within the Bullfrog Confining Unit (BFCU) very little transport was expected. To provide a better test for the code, additional simulations considered the source to be translated vertically upward to a location in the Calico Hills Vitric Tuff Aquifer (CHVTA).

The unclassified hydrologic source term used for these sources in the test problem was developed at Lawrence Livermore National Laboratory (LLNL) by Tompson et al. (1999) for CAMBRIC. Of the radionuclides modeled by Tompson et al. (1999), four radionuclides were considered, tritium, Sr-90, Pu-239, and Am-241. 2.04 moles of tritium were introduced instantaneously as a pulse. The other radionuclides entered the flow system as a time-varying flux as determined by Tompson et al. (1999). Tritium and Sr-90 were treated as non-sorbing. Pu-239 and Am-241 were assigned sorption coefficient (Kd) values of 50 and 100 liters/kilogram respectively. These values are consistent with the Frenchman Flat CAU model. Analysis of the BULLION Forced-Gradient Experiment (IT, 1998) suggested values of dispersivities of 10/3/2 m for longitudinal, transverse, and vertical directions

respectively. Since this experiment involved transport on the scale of 100 m, dispersivities were increased to 50 and 5 m for longitudinal and transverse directions for the Frenchman Flat CAU model. Consistent with the Frenchman Flat CAU model, dispersivities used for the Pahute Mesa test problem were 50 and 5 m.

The local geothermal gradient was included in the test problem for the two codes that account for temperature dependence. The value of the geothermal gradient used was 0.011 degrees Centigrade/m.

A.7.0 FRAC3DVS TEST

The development and evaluation of the FRAC3DVS model for the Pahute Mesa (PM) test problem is described in the following section. Details of grid development, incorporation of faults, and flow and transport results are provided. Following the results, the use of FRAC3DVS for the test problem is evaluated with respect to the testing criteria. The FRAC3DVS evaluation was done by an individual with considerable experience with this code.

A.7.1 Grid Development

Around the perimeter of the Pahute Mesa test problem nodes were located so that the heads or fluxes through faces would align directly with the regional model, thus simplifying input of either type of boundary condition from the regional model. Subdivisions around the perimeter of the Pahute Mesa test problem were made at 300-m intervals within the 1,500-m cell spacing of the regional model. Within the PM model limits, a regular grid of nodes at 300-m spacing was constructed using eV. This base array of nodes was then altered along the faults so that at 300-m distances along each fault trace a set of nodes 1-m apart were added. These 1-m node sets straddle the fault. Within 1.6 km of the tests SCOTCH and SERENA the node array including nodes straddling a fault were refined to 150-m node spacing. Within one km of the two events the nodes, including fault node sets were further refined to a 75-m spacing. The nodes were triangulated using Groundwater Modeling System (GMS) and edited so that the 1X300/150/75 m two-dimensional (2-D) elements straddling a fault corresponded correctly to the fault traces. The vertical spacing of nodes varied in the grid and the number of layers varied from 22 to 33 depending on the simulation. The number of nodes and elements also varied depending on the simulation.

In order to accommodate the requested vertical faults, the non-vertical offsets in the base PM geologic Voxel model had to be edited. This conversion was labor intensive and required hand editing of hydrostratigraphic layer top elevations at nodes near or on a fault to lower the geologic model (now converted to eV) in those areas. All layers were checked for inversions of layers, and

that a constant thickness of at least 1-m vertically was maintained in the geologic model layering. eV was then used to back interpolate from the areal model node array/mesh to the elevations on the 300-m eV geologic model layers resulting in definition of the easting, northing, and elevation for each node for each layer in the finite element model mesh. GMS was used to stack the 3D slices representing each hydrostratigraphic layer into FRAC3DVS input format. This completed the initial mesh generation.

A.7.2 Model Properties

A combination of eV and GMS was then used to assign the hydraulic properties to each prismatic element in the completed mesh. This was accomplished by using the eV geologic model of the area and lowering the 1-m thick portions of the base Voxel grid that represent areas where a unit is absent to an elevation slightly lower than the next unit encountered vertically. This was easily accomplished using the eV formula processor and yielded a “clean” (no 1-m spacer units) geologic model of the area. The eV model geologic units, called zones, were then removed one by one to reveal what geologic unit actually occupied the 1-m thick spacer sections of the grid. A *.tiff format figure was made for each layer and imported into GMS as a backdrop from which to assign the correct hydraulic properties to the elements in each flow and transport model layer.

Discrete faults/fractures can be defined within FRAC3DVS in three ways: (1) as an element face with an aperture width (fracture based equations); (2) as an element face with a hydraulic conductivity (fracture based equations); and (3) as a thin element with a high or low hydraulic conductivity (fracture flow approximated). This allows great flexibility in defining faults that, in reality, may be discrete faults/fractures, breccia zones, or otherwise acting as flow barriers or conduits.

The FRAC3DVS preprocessor NP is used to select which faces are chosen by defining the fault traces as selection criteria for the faces in the mesh. Properties such as aperture width for sets of faces are also input.

A.7.3 Boundary and Initial Conditions

Two types of boundary conditions were implemented in the test model, constant head (type 1) and flux (type 3). The constant head boundaries were used around the perimeter of the test model and

were defined areally and vertically from the MODFLOW regional model simulation after incorporation of the Pahute Mesa revisions. The assignment of the perimeter constant heads was done using eV. First the regional model head distribution at the block centered node locations was input as a data set to eV and a high density interpolated grid was generated. The locations of the PM model perimeter nodes were then input and the heads at these finite element locations were backinterpolated from the gridded regional model head distribution.

Constant flux boundaries were used to represent areal recharge to the model. eV was used to convert the flux from the regional model input data for input to the PM test model. GMS was used to select the element faces and assign fluxes for the test model element faces corresponding to the mapped recharge distribution from the eV 2-D regional model based grids. The GMS preprocessor then directly outputs the files required to run NP and FRAC3DVS.

A.7.4 Simulation Results

Flow

A noncalibrated simulation was made using the predesignated hydraulic conductivities for each unit, and a fracture aperture width of 0.00005 m for all faults except the North Timber Mountain Moat fault, which was set to 0.000001 m. It is important to note that no calibration effort was made to match the regional model results.

Radionuclide Transport

High constant concentration sources (1,000 kg/m³) with no retardation or decay were specified at the location of the SERENA and SCOTCH tests in order to test the areal and vertical numerical stability/dispersion in the transport model. The sources were specified at a number of model nodes (on the order of 10 per test) roughly corresponding to the location of the test cavities. Simulations of 1,000 years were conducted.

Numerical dispersion was not observed. Numerical stability was good; only small negative concentrations (typically < 5kg/ m³) were predicted areally and vertically at nodes along the periphery of the modeled plume. Beyond these nodes, alternating bands of very small positive and negative

concentrations were present. The solute mass balance error ranged from ~3% at 1 year to ~10% at 1,000 years.

High constant concentration sources (1,000 kg/m³), with no retardation or decay, were specified at a location in the aquifer unit (CHVTA) above the SCOTCH test and near the water table above the SERENA test in order to test the areal and vertical numerical stability/dispersion in the transport model. The sources were specified at a number of model nodes (on the order of 10 per test) roughly corresponding to the location of the test cavities. Simulations of 1,000 years were conducted. Numerical dispersion was not observed. Numerical stability was good; only small negative concentrations (typically < 5kg/m³) were predicted areally and vertically at nodes along the periphery of the modeled plume. Beyond these nodes, alternating bands of very small positive and negative concentrations were present. The solute mass balance error ranged from <1% initially to ~5% by 75 years to ~100% by 1,000 years. The error in mass balance is due to transport above the water table as the model was run in saturated mode.

Low constant concentration sources (2.0 x 10⁻⁷ kg/m³) with no retardation nor decay were specified at a location in the aquifer unit (CHVTA) above the SCOTCH test in order to test the areal and vertical numerical stability in the transport model. Simulations of 1,000 years were conducted. The simulated concentrations grade down over several orders of magnitude moving away from the source. Beginning at the periphery of the modeled plume and moving outward, alternating bands of very small positive and negative concentrations were present. Solute mass balance errors ranged from less than ~0.01% initially to ~2.5% at ~200 years to ~100% at 1,000 years.

In the simulations with sources in the aquifer units, transport was observed from source nodes upward to nodes where the nodal elevations exceed the calculated heads. To address this, simulations were attempted in variably, rather than fully, saturated mode. Once in variably saturated mode, difficulties were experienced in achieving flow field convergence. The authors of the code have suggested that the flow field may converge better if the variably saturated parameters are specified using the van Genuchten function option rather than using the tabular data option. This suggestion has not yet been implemented.

Tritium sources for the SERENA and SCOTCH tests corresponding to the LLNL unclassified hydrologic source term (Tompson et al., 1999) were specified at a number of model nodes (on the

order of 10 per test) roughly corresponding to the location of the test cavities. Initial concentrations were designated for these nodes so as to yield a total initial mass in the system of ~ 0.006 kg (2.0 moles), consistent with the LLNL hydrologic source term described in [Section A.6.0](#).

To determine the mass balance error, the computed nodal mass change for a given time step (i.e., the 'ins' and 'outs' at various types of boundary nodes) is compared to the change in mass stored in the domain for that time step (calculated from the total mass in the system at the end of the time step minus the total mass in the system at the beginning of the time step). For the tritium simulations, the first term was essentially zero ($\sim 1 \times 10^{-12}$ kg) throughout the simulation, as there is no further mass input after the initial pulse and the initial pulse does not reach any model boundaries. The second term (the change in mass stored in the domain for the time step) was typically 1×10^{-5} to 1×10^{-7} kg, depending upon the time step size. Comparing these two terms (1×10^{-12} vs. 1×10^{-7}), the mass balance error is large (5 orders of magnitude). However, as a percentage of the mass in the system, these masses are small. The change in mass stored during any given time step was typically 2 to 3 orders of magnitude less than the mass in the domain at the beginning of the time step.

Numerical stability was not adequate. Moving areally and vertically away from the source, nodal concentrations oscillated between positive and negative values. Altering timestep size did not have any effect towards correcting the output.

Pu-239, Am-241, and Sr-90 sources for the SERENA and SCOTCH tests were specified as one model node per test, with the node location roughly corresponding to the bottom of the test cavities. The sources were specified so as to approximate the pre-designated mass flux profile of the LLNL unclassified hydrologic source term (Tompson, et al., 1999). FRAC3DVS does not currently support specification of constant solute flux nodes in the interior of the model domain (the authors indicate that this can be remedied, but were unavailable to do so for these simulations). Consequently, the desired mass flux was approximated using multiple panel constant concentration source nodes. The concentration was increased relatively quickly in the beginning of the simulation and then slowly thereafter to approximate the desired mass flux profile for each of the three solutes. The solute mass balance error was typically 0.1% to 1.0% per time step.

Numerical stability was not adequate. Moving areally and vertically away from the source, nodal concentrations oscillated between positive and negative values as discussed above for tritium.

A.7.5 Performance Evaluation

Portability

The preprocessor GMS and codes NP/FRAC3DVS can run on both Personal Computer (PC) and UNIX based machines. The computer should have a fast processor (e.g., Pentium II 300MHz or faster) and have 256 Mb of RAM. The earthVision software runs only on UNIX based platforms to date, however within a year the eV software will be ported to PC based machines.

GMS is available free to government projects. The NP/FRAC3DVS software and source code is \$3,000. The earthVision software is very expensive to purchase (\$70,000+) but can be leased. For most applications involving a calibrated model and its review the use of earthVision is not necessary. It is only during the model construction phase that eV is extremely helpful.

QA Evaluation

All codes have been verified and documentation of the comparisons are included in the software user manuals.

Ease of Use

The FRAC3DVS code itself is a moderately difficult code to use. With the proper preprocessors the code is much more manageable. The input files for NP the pre-run processor are in ASCII format and therefore easy to check and manipulate if necessary. International System (SI) units are preferable for input structure, however other units can be used as long as they are dimensionally appropriate. GMS and eV are very user friendly and require only the self-tutorial to become familiar with the rudiments of the software.

Ability To Represent the CAU Hydrogeology

The FRAC3DVS code can simulate all of the pertinent hydrogeologic features of the mesa area and has good flexibility to represent faults in three ways. The code also has the built-in ability to generate random fractures/faults within the model for variability assessments. The code does not currently have the ability to do nonisothermal-based calculations, but the authors could add this feature given about six months to a year.

Speed of Simulation

Transport simulations on a Pentium II 300 MHz machine for one radionuclide in a steady-state flow field take one to two hours depending on the timestep size. The time required for a steady-state flow simulation is less than six hours, but is highly variable due to various factors such as good starting heads and variable saturation parameters.

A.8.0 SWIFT-98 TEST

The development and evaluation of the SWIFT-98 model for the Pahute Mesa test problem is described in the following section. Details of grid development, incorporation of faults, and flow and transport results are provided. Following the results, the use of SWIFT-98 for the test problem is evaluated with respect to the testing criteria. The SWIFT-98 evaluation was done by an individual with considerable experience with this code.

A.8.1 Model Assumptions

For the code comparison, a Pahute Mesa submodel was constructed based on Dirichelet (constant-head) boundary conditions interpolated from the MODFLOW regional model. For simplification, properties within each formation were assumed to be homogeneous. Radionuclide sources were defined in the vicinity of the SERENA and SCOTCH tests using source terms based upon the LLNL unclassified hydrologic source term model (Tompson, et al., 1999). The SWIFT-98 model was modeled as a water-table aquifer, which allows for nonlinear updating of transmissive and storage terms. The flow system was assumed to be at steady-state over the time-scale of the transport analyses. The base-case was simulated under isothermal conditions. Since large-scale faulting represents a major control on the flow system, two separate flow models were considered. For the SWIFT-98 simulations, the first model implements the fault effects, explicitly, by revising the hydraulic conductivities in each block that the fault traverses. The second model does not consider separate properties for fault blocks. Note that to some degree, faulting is considered, implicitly, since the geometry of the geologic model is also a function of the faulting.

A.8.2 Grid Development

The Pahute Mesa finite-difference grid used in the SWIFT-98 simulations, contains 224,952 rectangular prismatic blocks and is discretized into 103 columns, 104 rows and 21 horizontal layers. Spacings of the grid in the X and Y directions ranged from 75 m near the sources to 300 m on the

boundaries. The block elevations and thicknesses are equivalent to those used in the regional model. Vertical spacing was 150 m at the source elevations.

The northwest corner of the grid is located at the UTM easting and northing coordinates of 542772 and 4132833 m, respectively, and the grid is rotated 5 degrees clockwise at that corner. The top of the model is at an elevation of 2,000 m above mean sea level (amsl).

A.8.3 Model Properties

Flow

The porous media and fracture-zone hydraulic-conductivities used for all the models in the code comparison are described above in [Section A.6.0](#). The exact nature of the application of the properties and property-zones differs for each code. For the SWIFT-98 simulations properties were generated separately for each model block using a FORTRAN-90 pre-processing code, GEO2MOD.for, which uses the Pahute Mesa hydrogeologic model to assemble data files for the simulation model. The hydrogeologic model defines the surfaces for each of the HSUs at the site. GEO2MOD uses the HSU geometry comprising the geologic model in conjunction with a zone file (allowing for varied properties within each HSU) and property files defining properties for each zone within each HSU to assemble the input files for SWIFT-98. A vertical profile of HSU thicknesses is generated at simulation-block centers and properties are then generated assuming parallel combinations of horizontal properties for each block and series combination of vertical properties for each block (i.e., hydraulic conductivities). For isotropic properties (i.e., storage coefficients), an arithmetic average is used). GEO2MOD also considers the influence of faults and fault zones by combining fault properties with the porous media properties generated from the geologic model. Fault properties are combined in parallel to porous-media block properties in the direction of the faults and in series perpendicular to the fault. The trace of all faults is assumed to follow a path from block center to block center parallel (or perpendicular to the block faces). For SWIFT-98, the end product of the GEO2MOD simulation is a binary R1-21 input-card type file (Ward and Benegar, 1998). The faults were explicitly modeled as 20 m wide zones with hydraulic conductivities of 75 m/day.

Radionuclide Transport

Except for porosity data, which are assembled using GEO2MOD as described above, the solute-transport properties, assumed to be homogeneous in these code-testing efforts, are included in the main ASCII input file. The longitudinal and transverse dispersivities used in the simulations were 25 m and 2.5 m respectively. The molecular diffusivity, which includes the effects of diffusion and tortuosity, used in the simulations was 1.3×10^{-10} m²/s. A description of the source terms for the four radionuclides can be found in [Section A.6.0](#).

A.8.4 Model Boundary and Initial Conditions

Flow

The lateral boundaries of the numerical model are defined using SWIFT-98's steady-state aquifer influence functions (AIF). The steady-state AIF boundary conditions represent an additional flux term added to the finite difference equations that is based upon the hydraulic-gradient between the unknown block pressure and a user-given pressure applied to the outer block-edge and the block transmissivity. The boundary pressures used are based on the linear interpolation of hydraulic-heads generated by the regional MODFLOW model. SWIFT-98's infiltration option was used to apply infiltration to the surface of the model equivalent to that applied in the regional model. The infiltration was apportioned to the blocks based upon the position and surface area of local-model blocks relative to the regional model blocks.

Since the flow simulations were steady-state, the initial conditions were only needed to define the initial transmissivities used in the iterative solution of the non-linear water-table option. The initial condition used to define the flow system was assumed to be static with the water table located at the top of the model.

Radionuclide Transport

For solute transport, the steady-state AIF boundary conditions represent an additional advective flux term added to the finite difference equations. For boundaries with water leaving the system, the flux term is based upon the amount of mass that would be advected out of the system with that water. Water entering the system is assumed to have negligible contaminant concentrations (Reeves et al.,

1986). SWIFT-98's infiltration option assumes water entering the system is clean. For the radionuclide transport, the initial concentrations in the system were considered to be negligible.

A.8.5 Simulation Results

Flow

Two separate steady-state flow models were considered in the simulations. The first model explicitly considers the influence of the faults on the flow-field, by updating the hydraulic conductivities in any blocks traversed by faults. The second model does not include updated conductivities for the fault blocks. For purposes of testing, the inclusion of fault blocks assumed the highest hydraulic conductivity in the expected range allowing a check on the influence of high-velocity zones on the codes ability to efficiently solve the problem. The results showed the marked degree of influence that the fault blocks have on the flow system. The faults are acting as conduits and obscure some of the features of the flow field generated by heterogeneities as reflected in the geologic model.

Radionuclide Transport

Four sets of radionuclide transport simulations were performed using SWIFT-98 in the code comparison. Simulations were performed using each of the two steady-state runs and two different source conditions. For all the SWIFT-98 simulations, the SERENA source was placed in the third layer, but the SCOTCH source was simulated in the third layer for half of the runs and in the fifth layer for half of the runs. The actual working point elevation would place the SCOTCH source in the fifth layer but it was of interest to see how much change in results and solution efficiency would occur if the source was moved from a low conductivity to a higher conductivity zone. Results are presented for the following cases:

- Case 0: Explicit-fault model with the SCOTCH source located at its working point in layer 5,
- Case 1: Explicit-fault model with the SCOTCH source translated vertically upward to the aquifer (CHVTA) in layer 3,
- Case 2: No-fault model with the SCOTCH source located in layer 5,
- Case 3: No-fault model with the SCOTCH source translated vertically upward to the aquifer (CHVTA) in layer 3,

Simulations were performed for the four radionuclides tritium, Am-241, Pu-239 and Sr-90. In total a combination of 16 transient transport simulations were performed using SWIFT-98. Mass balance errors for all simulations were less than 0.01 percent.

Simulation results were compared graphically at 50, 100, and 200 years for all radionuclides and for Am-241 and Pu-239 at 1,000 years. Note results for tritium and Sr-90 at 1,000 years are not considered due to their short half-lives.

Fault-controlled transport for tritium leaving the SERENA site was observed and the lesser spreading of tritium from the SCOTCH site which is located in a lower, less conductive layer further from any fault zones. With fracture flow and decay there was relatively rapid dissipation of the tritium mass from the SERENA site over 100 years. The SCOTCH source tritium levels also show the effects of decay, but are not as influenced by the dilution effects associated with the fault controlled spreading. When the source is placed in layer 3 there is a marked increase in horizontal transport for the SCOTCH source. The increased horizontal transport in the upper layers also combined with the vertical mixing to create a mechanism for a farther distribution of mass in layer 5.

When faults are not included, the tritium transport is more contained than when the faults are explicitly modeled. The need to examine the nature of the fault zones in Pahute Mesa is seen. When the SCOTCH source is moved up into the third layer the degree of spreading increases for the porous-medium (no-fault) model. This is indicative of the need to examine the vertical flow in the source areas.

The pattern for Sr-90 distribution at 50 years is similar to that for the tritium transport, but the more long-term nature of the source and the lesser quantities of material tend to accentuate the degree of fault control of the transport. When the source is moved up to the aquifer, spreading increases.

Little transport is noted at 200 years for Am-241 for Case 3 and 1,000 years for Pu-239 due to the strongly absorptive nature of the radionuclides. Results are similar for all times and cases for these two species.

In addition to simulating Case 3 with the four test radionuclides, Case 3 was also simulated for a conservative (non-decaying and non-sorbing) species subject to matrix diffusion. This allowed for

testing of the dual-porosity option in SWIFT-98. SWIFT-98 also has a dual-permeability option, but since matrix-diffusion is the process of concern, advection in the matrix was ignored in these simulations. The parallel fracture option of the code was used. The matrix blocks were considered to be 2.5 m apart. Two cases were simulated, one using an effective diffusivity of 3×10^{-11} m²/s, and the second using a diffusivity of 0, for comparison. The potential retarding effects of matrix-diffusion was verified in these simulations.

A.8.6 Nonisothermal Test

In order to test flow and transport under nonisothermal conditions, a test problem was designed that included the local geothermal gradient. There was some difficulty with the nonisothermal model translating the heads from the isothermal MODFLOW model to the boundaries of the nonisothermal model. After numerous attempts to obtain a steady-state flow field failed, this test was abandoned. The problem of taking a head from an isothermal model and mapping it in as a boundary condition for a nonisothermal model is discussed further in [Section A.9.0](#).

A.8.7 Performance Evaluation

Portability

The SWIFT-98 code is designed to run on Pentium processors. This version is specifically designed for use in conjunction with the Lahey LF90 Fortran compiler. Since a compiled version of the code is available, the user does not need to have this compiler unless his problem dimensions exceed the present dimensions of the code. The Pahute Mesa test problem needed 256 MB of RAM to avoid paging. The associated pre- and post- processors are also designed to run on Pentium processors. The only restriction on these codes involves GEO2MOD, which generates a binary input file for SWIFT-98 and would need the Lahey LF90 Fortran compiler for compatibility if recompilation was necessary. All the other codes could be compiled with any Fortran compiler. As with SWIFT-98, compiled versions of the pre- and post-processors are available. Results of the simulations are saved in ASCII map files which can be converted to a format that can be used in any standard contouring package. For this study, *.CSV (comma separated variables) files that can be used in conjunction with SURFER for Windows were generated by one of the post-processing codes. Window-based EXCEL macro programs were then used to plot the results of simulations from the *.CSV files. The macro programs need to be run on a PC containing Excel and Surfer.

QA Evaluation

The SWIFT genre of codes have undergone verification and field comparison (validation) testing during their development and maintenance by Sandia National Laboratories (Ward et al., 1984). SWIFT-98, which is maintained by HSI-GeoTrans, Inc., has also undergone the same testing procedure as described in Ward et al. (1984). Additionally, all changes made to the code have been tested. The testing was concluded March 1998. All test problems are included on the CD release of the code.

Ease of Use

SWIFT-98 is a difficult code to use, relative to standard groundwater flow and solute transport such as MODFLOW/MODFLOWT. The major difficulties are associated with the rigorous nature of the code, which allows the user to couple density-dependent heat and brine transport with the groundwater flow model. In addition, the user's manual is sometimes unclear as to input needed, but the documented sample problems help (Ward, et al., 1984). Still, for a fully coupled model, the model would probably have to be considered average in difficulty of usage. Some observations noted during this project and the Frenchman Flat modeling project are mentioned below.

Because most of the solute transport parameters needed for radionuclide transport in a steady-state flow field are required in the steady-state flow data set, SWIFT-98 is not always amenable to performing multiple transport simulations based on a single steady-state flow simulation. For problems where the steady-state flow simulation takes an excessive number of iterations to converge, the need to rerun the flow problem for different sets of transport parameters in the same flow-field is inefficient. This can be a problem since upwards to 100,000 iterations may be need to solve a 3-D isothermal flow problem when the system is extremely heterogeneous and the boundary conditions are mainly flux boundary conditions. SWIFT-98 was updated to allow for a change in half-life and absorption coefficient for each transport simulation. This update was easy to implement in the code because these parameters are used in assembling the equations each time step. For parameters such as dispersivity the terms are assembled in conjunction with the steady-state flow run and used as composite terms thereafter (even in restart runs). Updating SWIFT-98 to reassemble the composite terms would be a more difficult procedure. For complex 3-dimensional problems where heat flow is considered, boundary conditions other than no-flux and infiltration must be generated from

larger-scale simulations. Field-study based temperature and pressure profiles from which boundary conditions for the coupled thermal problems can be derived are unlikely to be available.

Implementation of the dual-porosity mode in SWIFT-98 is quite easy.

Ability To Represent CAU Hydrogeology

SWIFT-98 is a block-centered finite-difference program and as such is not as flexible in its ability to explicitly incorporate the geometric aspects of the Pahute Mesa geologic model as some finite-element models (i.e., reproducing the shapes of the individual HSUs). Note that this is not true of finite-element models with the assembled equations directly integrated (as opposed to numerically integrated). Finite element codes, which utilize pre-spatially-integrated rectangular prismatic elements, would tend to be no more flexible in defining the geometry of the system than SWIFT-98. With SWIFT-98, the rectangular prism-type blocks can be defined by rows, columns and horizontal layers or in a stair-step fashion by rows, columns, the top elevation of the uppermost block of column i and row j , and the thickness of each block in column/row (i, j). The latter method allows for flexibility in defining the layering of a system, but not the discretization in the plan view. In the plan-view, all blocks along a column or a row must have the same width. In our test simulations, the simpler horizontal layering scheme was utilized. The change of hydrologic properties with depth as defined by HSU's was implicitly considered in block properties. When a block contained material from more than one HSU, a composite property was generated using a preprocessor. The process worked quite well as could be seen by comparing the SWIFT-98 flow model results with the FEHM flow model results. The ability of this methodology to represent the influence of the HSU heterogeneities and fault structures was seen in the SWIFT-98 results.

Speed of Simulation

[Table A.11-2](#) contains a compilation of simulation CPU times for the flow and transport runs. The steady-state flow simulation of the explicit fault model took 23.4 minutes to solve as opposed to 13.1 minutes to solve the “no-fault” flow simulations. These results show that explicit inclusion of faults reduced the efficiency of the L2SOR solver. It should be noted when comparing the solution times to those for the other codes, that the SWIFT-98 simulations also included nonlinear iterations used to adjust physical properties that are a function of the water-table position.

For transport, the differences in simulation times are a function of the number of time steps used in the analysis and the number of linear iterations used in the indirect L2SOR solution scheme. The time stepping schemes used in the Am-241, Pu-239 and Sr-90 analyses were all the same. This was only for convenience, as much larger time steps could have been used for the Pu-239 and Am-241 analyses due to the slower retarded velocities. The short half-life of tritium dictated a need for a smaller time step in the analysis. The time stepping scheme used for the other species generated an oscillatory behavior in the tritium runs that obscured the concentrations at a level of interest.

As can readily be discerned from [Table A.11-2](#), the tritium simulations were slower than most of the other simulations. The solution time was longer for Sr-90 with the source in layer 3 than Sr-90 with the source in layer 5, but the positioning of the SCOTCH source in layer 3 markedly slows down the solution process. The slow rate of solution for Sr-90 is due to an increased number of iterations needed for convergence.

A.9.0 FEHM TEST

The development and evaluation of the FEHM models for the Pahute Mesa test problem is described in the following section. Details of grid development, incorporation of faults, and flow and transport results are provided. Following the results, the use of FEHM for the test problem is evaluated with respect to the testing criteria. The FEHM evaluation was done by an individual with only minor previous experience with this code applied to small one-dimensional flow problems. The time required to set up and run the models for the test problem included training.

A.9.1 Model Assumptions

Flow

Assumptions for the flow and energy transport models discussed by Zyvoloski et al. (1997b) include fluid flow governed by Darcy's law, thermal equilibrium between fluid and rock, immovable rock phase, and negligible viscous heating. An additional assumption not required by the FEHM code but imposed on the test problem was modeling the test problem as a confined aquifer.

Radionuclide Transport

General assumptions discussed by Zyvoloski et al. (1997b) for the reactive transport model are summarized here. Concentrations of solutes are assumed to be low enough that their presence does not affect the properties of the fluid or the flow fields. Chemical reactions do not influence the energy balance and reactions between fluid and solid phases do not affect the hydrologic properties of the rock. Specific assumptions are discussed further by Zyvoloski, et al. (1997b).

Transport in FEHM can be simulated with either finite-element continuity equations (advection-dispersion-reaction equations) or with either of two particle tracking models. With the continuity approach, full reactive transport of multiple interacting reactive solutes can be simulated with either a single or dual continuum model formulation. In the particle-tracking model in the version of FEHM tested, matrix diffusion is solved with a semi-infinite boundary condition between

the fractures. This approach is limited to conditions where the diffusion distance is small with respect to the fracture spacing. A newer version of FEHM recently released incorporates finite fracture spacings into the particle tracking modules to more accurately simulate diffusion when distances between fractures is small.

Additional assumptions not required by the FEHM code but imposed on the test problem include the assumption that the flow system is at steady-state for the transport simulations and that the matrix porosities and fracture volume fractions are homogeneous within a hydrostratigraphic unit. In addition, linear distribution coefficients are dependent only on the radionuclide, and molecular diffusivities and dispersivities are constants, independent of radionuclide or hydrostratigraphic unit. The LLNL unclassified hydrologic source term developed by Tompson et al. (1999) discussed in [Section A.6.0](#) was used at each source location.

A.9.2 Grid Development

Grid Generation Tools

Computational mesh generation tools for this model include the LaGriT Los Alamos Grid Toolbox (George, 1997) suite of grid meshing tools. Developed at LANL, this software provides an integrated system for all grid generation steps, from initial model import, to quality checking and postprocessing of input data, mesh optimization, 3-D mesh post-processing and quality checking, and mesh interfacing with the FEHM flow and transport code, and fault property inclusion into the model.

LaGriT is a library of user callable tools that provide mesh generation, mesh optimization and dynamic mesh maintenance in three dimensions for a variety of applications. Geometric regions within arbitrarily complicated geometries are defined as combinations of bounding surfaces, where the surfaces are described analytically or as collections of points in space. A variety of techniques for distributing points within these geometric regions are provided. Mesh generation uses a Delaunay tetrahedralization algorithm that respects material interfaces and assures that there are no negative coupling coefficients. A specialized subset of LaGriT has been developed specifically for hydrogeologic applications. The LaGriT code is documented in LaGriT User's Manual, LA-UR-95-3608, and maintained online at www.t12.lanl.gov/~lagrit.

Input Data - Surfaces

All grids for the test model are built using the Bechtel Nevada hydrogeologic model of Drellack and Prothro (1997). Whereas the test model is rotated 5 degrees from UTM coordinates to coincide with the MODFLOW regional flow model, the Bechtel Nevada hydrogeologic model is not rotated. The finite-element grid is generated from a point distribution associated with the tops of each HSU, so a new point distribution for each HSU was generated to be consistent with the rotated test domain. The test problem point distribution consists of a rectangle with the corners NW (542909.12, 4132671.15), NE (563530.36, 4130867.03), SE (561856.97, 4111740.08), SW (541235.73, 4113544.2) with 300 m spacing. The entire set of points is a rectangle translated 5 degrees off the x-axis.

The input surface files for the model are created using the test problem point distribution, a ray-shooting technique, and contoured surface files of HSUs in the Pahute Mesa area as developed by Drellack and Prothro (1997). To create a new surface, the test problem point distribution is positioned above a HSU surface and rays are projected through each x,y point on to the HSU surface to find the elevation for each point. This is done with each HSU surface to create the x,y,z coordinate points for each test problem surface. The points are then connected into triangular elements, creating a Triangular Irregular Network (TIN) for each surface of the test problem. Each surface is represented by a TIN sheet of 4,550 x,y,z coordinates and the connectivity for 8,832 triangles.

Input Data – Refinement and Quality Checking

For this model, there are two regions with increased grid resolution representing SCOTCH and SERENA sites. SCOTCH is represented with the x,y polygon with corners at (554833., 4124400.), (556626., 4124243.), (554990., 4126193.), (556783., 4126036.). SERENA has corners at (548714., 4126742.), (550507., 4126585.), (548897., 4128834.), (550690., 4128677.). Each TIN surface for the test problem is refined so that each site has elements of edge size 75 m, surrounded by a transitional buffer with elements of size 150 m. The remaining elements have edge size of 300 m. The final test problem refined surface has 5,275 points and 10,282 triangles. The surface files are tested to ensure that there are no holes, that no triangles overlap, and all triangles are ordered to have their normal vector on the same side of the TIN.

Building the 3-D Tetrahedral Mesh-Create Volumes Between Surfaces

The 3-D model is developed by effectively stacking all the contoured surfaces and populating the volume between the layers with test problem attributes. The TIN sheets are stacked from lowest elevation to highest elevation. The volumes between the surfaces are converted to prism elements (6 nodes, 2 triangle faces, 4 quadrilateral faces) with vertical connections between adjacent layers. Each prism is converted to three tetrahedra so that the final representation is in the form of a 3-D tetrahedral mesh.

Building the 3-D Tetrahedral Mesh-Refinement and Quality Checking

In preparation of a computational grid, thick units are subdivided vertically to provide a more gradual transition to the thinner layers, and to keep the horizontal edges in proportion to the vertical edges. The interfaces are buffered by a lower and upper surface of a distance of 15 m to be able to capture the unit geometry with Voronoi cells after the computational grid is created. A minimum unit thickness of 14 m is chosen so that large aspect ratio tetrahedral and triangular elements are avoided. The grid is checked to ensure there are no holes, and that the geometry correctly represents the Bechtel Nevada hydrogeologic model.

Delaunay Computational Grid

Numerical solution techniques for flow and transport calculations with finite volume and integrated finite difference methods place geometric constraints on the quality of a mesh. To optimize the mesh, reconnection algorithms enhance the quality while preserving the geometry. Reconnection can be done without adding points by allowing connections to flip. In the final mesh, points may be added or removed as needed to create a Delaunay grid with positive coupling coefficients.

The FEHM flow and transport code uses finite volume control volumes for solution of flow and transport equations. Part of the grid generation process is to calculate the Voronoi control volume associated with each node in the grid and the area of the polygonal faces of the Voronoi control volumes. In addition to control volumes, lists are created containing the surface area of each node on the surface of the grid, for use in scaling constant flux boundary conditions. Node sets for each material property are also written, including outside, top and bottom locations for each node.

The final Delaunay computational grid for 3-D calculations contains 138,680 nodes and 839,289 tetrahedral elements and accurately represents the geometry of the Bechtel Nevada hydrogeologic model.

Fault Zones

For the test model, a method developed by LANL was used to model the intersections of fault zones with the predetermined stratigraphy. The new capability provides a way to create fault planes from the surface maps of faults. This routine has the ability to offset a surface map of faults and to connect the original and offset maps to create a fence diagram defined by two-dimensional elements. The offset can be arbitrary, allowing for angled faults or for faults that have moved multiple times in different directions creating a new catalog of elements in the fault zones. In an unstructured grid, the width of the fault zone will vary depending on local resolution. The new routine gives LaGriT the capability to find the intersection of a grid containing two-dimensional elements representing the faults with the stratigraphic grid of tetrahedral elements and catalog which elements (if any) are intersected. This procedure is well documented, and is relatively robust.

A.9.3 Model Properties

Flow

The FEHM model consisted of 22 HSUs. The nodes in a given zone were assigned parameter values for hydraulic conductivity, fracture volume fraction, and porosity. Nodes assigned to faults were given a hydraulic conductivity of 75 m/day consistent with the highest value of the range estimated for fault conductivity. Isotropic hydraulic conductivities were used for the isothermal models and anisotropic hydraulic conductivities for the nonisothermal model.

Radionuclide Transport

The hydrologic source term is described in [Section A.6.0](#) as well as values used for linear sorption coefficients and dispersivities. Source locations for simulations were chosen for each test as the node closest to the working point of the SCOTCH and SERENA tests. The SERENA working point is located in the Calico Hills Zeolitized Composite Unit (CHZCM). Since the location of SCOTCH is within the Bullfrog Confining Unit (BFCU) very little transport was expected. To provide a better test for the code, additional simulations considered the source to be translated vertically upward to a

node in the Calico Hills Vitric Tuff Aquifer (CHVTA). An additional scenario considered in the FEHM test kept the SCOTCH source in the BFCU and prescribed a high permeability chimney extending upwards to the water table.

A.9.4 Boundary and Initial Conditions

Flow

The lateral boundaries of the model were set as specified head boundaries. Values of hydraulic head from the MODFLOW regional model for the test problem area were obtained as described in [Section A.6.0](#). A simple approach was taken for mapping the MODFLOW regional model heads onto the boundaries of the test problem. For every MODFLOW regional model cell along the boundaries of the test problem area, the value of the steady-state hydraulic head at the regional cell center was mapped onto the FEHM boundary nodes that were positioned within the borders of the regional cell face. The top (the water table) and bottom (top of the Pre-Tertiary unit) of the model were considered no-flow boundaries. For simplicity, recharge due to infiltration was not incorporated in the FEHM test but could be included as required. Initial conditions were set at a value of 1,400 m of head for every node in the grid. Simplified boundary conditions were used for the nonisothermal simulations imposing an approximately 200 m head gradient from north to south and no-flow boundaries on the east and west sides. Initial conditions were uniform fluid pressure and temperature distribution determined by a geothermal gradient of 0.011 degrees Centigrade/m.

Radionuclide Transport

For the FEHM test problem the concentration of solute in water entering the system was set to zero, but could be specified as a non-zero concentration. Internal sources can be specified as fixed concentration, instantaneous mass input, or time-dependent mass flux or concentration. For the test problem sources were specified as instantaneous mass input for tritium and as time-dependent mass fluxes for Am-241, Pu-239, and Sr-90.

A.9.5 Simulation Results

A number of situations were considered to provide a range of circumstances for testing the code. Five flow scenarios were considered and 14 transient transport simulations were performed. The number

of transport simulations could be reduced to 14 due to the ability of FEHM to treat multiple chemical species simultaneously. Mass balance errors for all simulations were less than 0.05 percent.

Flow

Five distinct steady-state flow models were developed for the FEHM test. These flow models were:

1. Isothermal, no faults
2. Isothermal, faults included
3. Isothermal, no faults, chimney included
4. Isothermal, faults included, chimney included
5. Nonisothermal, no faults, chimney included.

Inclusion of faults set to a hydraulic conductivity at the high end of the estimated range had a noticeable influence on the flow field. Presence of the chimney either with or without faults did not affect the flow field at the scale of the model domain.

Radionuclide Transport

Four sets of isothermal radionuclide transport simulations were conducted using an instantaneous injection of 2.04 moles of tritium as the source. These correspond to the first four steady-state flow models listed above; no faults, faults included, no faults chimney included, and faults and chimney included. Sources were located at the SCOTCH and SERENA working points and in the aquifer (CHVTA) above SCOTCH.

For the no fault case, tritium did not move far from the source nodes since the working points are located in low permeability units. When the source was moved up to the higher permeability unit, more movement occurred. The model captured the dissipation of tritium concentrations at 200 years due to decay. Time step control was checked to assure the accuracy of the simulations.

When faults were included at the maximum estimated permeability, simulations showed tritium moving from the SERENA cavity into the Boxcar Fault ([Figure A.11-1](#)) and away from the source. The sensitivity of transport to fault zone properties was evident. The effect of including a high permeability chimney above the SCOTCH working point was to allow tritium to move upwards from the confining unit into the permeable aquifer above. Once in the CHVTA, tritium spread downgradient.

The ability of the code to simulate multiple sorbing species simultaneously was tested by assigning the time varying fluxes of Sr-90, Am-241, and Pu-239 obtained from the LLNL unclassified hydrologic source term model to the nodes used for the SCOTCH and SERENA working points and the source in the CHVTA. Sorption coefficients were given to Am-241 and Pu-239; Sr-90 was treated as non-sorbing. Only the model that included faults was used. The first simulation considered all three radionuclides being injected at the SCOTCH and SERENA working points. At 50 years, little movement occurred for the sorbing radionuclides; however Sr-90 moved along the faults and downwards. Simulations for the three radionuclides at 200 years showed some small movement for Pu-239 and Am-241 with the shorter-lived Sr-90 concentrations decreasing due to decay. At 1,000 years, Pu-239 and Am-241 moved further along the faults and Sr-90 decayed away. Even when the source was moved upwards to the CHVTA, transport distances were small for the sorbing radionuclides. The non-sorbing Sr-90 moved several kilometers by 50 years but the front retreated at 200 years due to decay.

The capability of representing matrix diffusion processes was evaluated using one of FEHM's particle tracking models. Two simulations were conducted for comparison. In the first, a non-sorbing, non-decaying tracer was released in the CHVTA considering only advection and dispersion but not matrix diffusion. In the second, the same conditions were maintained but in addition, matrix diffusion was modeled. Results showed the code was able to represent the reduction of transport distance due to matrix diffusion. While not included in this evaluation, this particle tracking model does have additional options for sorption and decay. The particle tracking method is also used to represent colloid transport in fractured media.

A.9.6 Nonisothermal Test

In order to test flow and transport under nonisothermal conditions, a test problem was designed which uses slightly simpler boundary conditions than those used in the isothermal test cases. This is due to the effort that would have been required to convert isothermal heads to nonisothermal pressures. Because the density of water depends on its temperature, the conversion would have required several days investment in developing and testing a pre-processor. Therefore, a simpler case with a 200m head gradient north to south and 0.011 degree/m geothermal gradient was specified. A steady-state pressure and temperature field was obtained from the simulation.

Transport under nonisothermal conditions was evaluated using the nonisothermal flow model for the case without faults but including a high permeability chimney extending upwards from the SCOTCH working point to the water table. Sources consisting of 2.04 moles of tritium injected instantaneously were located at the SCOTCH and SERENA working points. Tritium movement was greater as compared with the isothermal case possibly due to increased hydraulic conductivity with temperature.

A.9.7 Performance Evaluation

Portability

Computational mesh generation tools for this model include the LaGriT Los Alamos Grid Toolbox (George, 1997) suite of grid meshing tools. LaGriT is a library of user callable tools that provide mesh generation, mesh optimization and dynamic mesh maintenance in three dimensions for a variety of applications. LaGriT and associated applications require a UNIX based platform. The software, users manuals, and examples are available at no cost from LANL. However, since considerable training is required to use these tools effectively, the grid for this test was developed by staff at LANL. All transfers of data files were done electronically through e-mail attachments or the LANL ftp site.

FEHM is available for a number of platforms including PC. This test was conducted on a Dell Precision Workstation 610 with twin 400 MHz Pentium II Xeon processors and 1 GB of physical memory. A post-processor that runs on a PC is available to convert FEHM output files into a format readable by visualization software such as Tecplot.

QA Evaluation

The FEHM code continues to be subjected to an extensive verification and validation effort and is maintained in a software configuration management system. The verification and validation plan are provided in detail by Dash et al. (1997). The objective of the verification is to test the options and features of the code. This is accomplished by comparing the results of simulations with published analytical solutions and results from other codes. Every time a modification is made to the code, it is tested with a suite of verification problems to insure no errors were introduced or capabilities eliminated. Validation will include modeling of a number of field tests when data become available.

The tests considered in the verification effort are described in detail by Dash et al. (1997) and test results are discussed. A number of additional documents supporting the FEHM code are readily available from LANL. These documents include the user's manual (Zyvoloski, et al., 1997a), and a description of the mathematical models and numerical methods used by FEHM (Zyvoloski, et al., 1997b).

Ease of Use

As discussed above, grid development was done at LANL. The hydrogeologic model and coordinates for source zone refinements were transferred electronically from IT to LANL. The completed grid was transferred electronically back to IT. This process was efficient and LANL staff were responsive to requested modifications.

Since the FEHM test was conducted by an evaluator with only limited previous exposure to FEHM, the five flow models and the fourteen transport simulations presented above were completed with technical support from LANL by telephone. With the availability of LANL technical support, all the simulations presented in this section were completed in seven weeks.

The users manual for FEHM is clearly written describing in detail all the data files, input data, and output files and includes examples for many of the macro control statements. Combining the available documentation with some training and telephone access to an experienced user, FEHM is surprisingly easy to use.

There was little difficulty getting isothermal flow and transport models running. There was some difficulty with the nonisothermal model translating the heads from the isothermal MODFOW model to the boundaries of the nonisothermal model. This was the same problem encountered in the SWIFT-98 test and is not code specific. Namely, one cannot simply take a head from an isothermal model and map it in as a boundary condition for a nonisothermal model. This is due, in part, to the density variation with temperature. Since the non-isothermal model tested here uses a geothermal gradient of increasing temperature with depth, then the pressure at any depth on a boundary needs to account for the variation in density of the water above that location. A pre-processor could be written to effectively integrate the pressure for each nonisothermal model boundary cell. This would entail choosing a reference temperature for the isothermal model from which the boundary pressures are

interpolated. This problem could have been solved with an investment of several days work to write and test a pre-processor. However, for the purposes of demonstrating the nonisothermal capability of FEHM, it was more efficient to use simpler boundary conditions.

Ability To Represent the CAU Hydrogeology

The unstructured 3-D finite-element mesh provided by LANL accurately represents to the resolution of the hydrogeologic model the complex geometry and distribution of the hydrostratigraphic units for the Pahute Mesa test problem. Faults were included through a method that creates fault planes from surface maps of faults. The specific offset across a fault, however, is only as accurate as the resolution of the hydrogeologic model. Faults may be specified as non-vertical, although for comparability with the finite difference code SWIFT-98, vertical faults were used for the test problem. The finite-element mesh was further improved for the test problem to provide higher resolution in the source regions. In addition to the ability of the mesh generating tools to represent complex geometry, the ability of FEHM to represent other attributes and processes characteristic of the CAU hydrogeology were demonstrated in this evaluation. These are, the capabilities to simulate a 3-D system, heterogeneous and anisotropic hydraulic conductivity, point and distributed sources and sinks of water, advection, dispersion, sorption, matrix diffusion and temperature dependent flow.

Speed of Simulation

CPU times in minutes for flow, finite-element transport, and particle tracking transport simulations are shown in [Table A.11-3](#). Times for the steady-state flow simulations with or without faults were similar ranging from 15 to 19 minutes. Times for 200 year tritium simulations increased from 77 to 103 minutes when the source at SCOTCH was moved up to the CHVTA. Similar results were seen for the 1,000-year simulations of the simultaneous transport of three radionuclides, Am-241, Pu-239, and Sr-90. As anticipated, the particle tracking transport model was much faster.

A.10.0 CONCLUSIONS

The first criteria that must be met by the codes as a minimum standard prior to evaluating other criteria is whether or not plausible flow fields and transport results could be produced for the test problem. All three codes produced reasonable representations of steady-state flow fields, Differences between the codes became apparent for the transport simulations.

While FRAC3DVS shows promise for applications such as conceptual model testing of fracture-matrix interactions at smaller scales, difficulties were encountered applying the code to a problem of the scale used for this test. Problems with simulations of non-decaying, non-sorbing tracers included alternating bands of positive and negative concentrations and solute mass balance errors as high as 10 percent when the sources were modeled in confining units. When the source was translated upward to the aquifer unit, mass balance errors were as large as 100 percent due to the model simulating movement of the tracer into the unsaturated zone. The code authors have suggested that this problem could be resolved by using the variably saturated mode and specifying parameters for an unsaturated hydraulic conductivity model. This approach would increase simulation times and memory requirements. Simulations of an instantaneous pulse of tritium as specified by the LLNL unclassified hydrologic source term model showed significant oscillations between positive and negative concentrations. Since reducing the time step did not resolve the problem, the proposed solution is to further refine the grid down gradient from the source. This would increase the number of nodes required for the model. Simulation of the fluxes of Am-241, Pu-239, and Sr-90 from the working points revealed a previously unidentified limitation of FRAC3DVS. The current version does not support time varying solute flux at source nodes in the interior of the model domain. The code authors have stated that this limitation could be removed with further development. Considerable time was spent on this test problem by a modeler with significant experience. Using the LLNL source term, plausible transport results with acceptable mass balance were never achieved with FRAC3DVS. While these problems may be resolved with an investment of additional time and effort, the results of this test argue for eliminating FRAC3DVS from further consideration.

The results of SWIFT-98 simulations conducted for this test were satisfactory and demonstrated the required code capabilities. The only difficulty encountered was for nonisothermal conditions. The problem of translating boundary conditions from an isothermal model to a nonisothermal model was also experienced for nonisothermal simulations with FEHM. A pre-processor can easily be written to map the boundary conditions more accurately, as described in [Section A.9.0](#). The results of the FEHM simulations were satisfactory and demonstrated the required code capabilities.

Criteria set out for evaluating the codes were portability, QA evaluation, ease of use, ability to represent the CAU hydrogeology, and speed of simulation. Portability and the ability to represent the CAU hydrogeology are linked and will be addressed first.

Portability/Ability To Represent CAU Hydrogeology

A major difference between FEHM and SWIFT-98 is how the hydrogeologic model is represented by the computational grid. SWIFT-98 is a finite-difference program and, as such, is not as flexible as a finite-element model at capturing the geometric shape of the individual hydrostratigraphic units. The rectangular prism-type blocks used for the SWIFT-98 grid can be defined by rows, columns and horizontal layers or in a stair-step fashion by rows, columns, the top elevation of the uppermost block of column *i* and row *j*, and the thickness of each block in column/row (*i, j*). The latter method allows for flexibility in defining the layering of a system, but not the discretization in the plan view. In plan-view, all blocks along a column or a row must have the same width. In the SWIFT-98 test simulations, the simpler horizontal layering scheme was utilized. The change of hydrologic properties with depth as defined by HSUs was implicitly considered in block properties by averaging all of the different HSU properties contained in each finite difference block. When a block contained material from more than one HSU a composite property was generated using a preprocessor. The pre-processor also considers the influence of faults and fault zones by combining fault properties with the porous media properties generated from the hydrogeologic model. Fault properties are combined in parallel to porous-media block properties in the direction of the faults and in series perpendicular to the fault. The trace of all faults is assumed to follow a path from block center to block center parallel (or perpendicular to the block faces). The block structure of the grid does not allow for non-vertical faults.

The grid generation tools interfaced with the FEHM code allowed for the accurate representation of the complexities of the hydrogeologic model for Pahute Mesa. The hydrostratigraphic structure as provided by the hydrogeologic model was captured in the finite-element grid. This included units of variable thickness and units that pinch out. Faults were included through a method that creates fault planes from surface maps of faults. With this method the specific offset across a fault was only as accurate as the resolution of the geologic model. While faults for the test problem were vertical, faults may be specified as non-vertical. Higher resolution of the grid was provided in source and down gradient regions. The exact specification of hydrostratigraphic units eliminated the need to use composite properties in the model.

The tradeoff for the finite difference approach is that while there is a loss of resolution and an averaging of properties in some cases, the methodology used to develop the grid is easy to implement and is more portable. The finite-element approach using unstructured grids accurately represents the hydrogeologic model but at the cost of requiring sophisticated grid generation tools. However, FEHM can also be applied to simple structured grids; it is distributed with a structured grid generation program.

Given the available methods, portability and accuracy of representation of the hydrogeology appear to be inversely related performance measures. Methods for developing the model grid and assigning model properties that require only a PC and easy to implement software produce models that average hydrogeologic features and properties. Methods for producing accurate representations of the hydrogeology and assigning model properties more accurately require less common hardware and software capabilities. As such, the measures of portability and accuracy need to be ranked in terms of their relative weights in the decision process. This relative weighting can be interpreted from the discussion of modeling issues provided by the Frenchman Flat CAU model peer reviews. The reviews emphasized the need for modeling approaches that would provide accurate representation of hydrostratigraphic units, accurate representation of faults, higher grid resolution in source areas and accurate transport predictions.

For the purposes of this evaluation, the conclusions of the peer reviews will be considered valid and accuracy will be given more weight than portability. In that case, FEHM with a better ability to represent the CAU hydrogeology but less portability would be ranked above SWIFT-98 for these two

criteria. If the relative importance between portability and accuracy is reversed, a comparison of FEHM and SWIFT using only simple, structured grids would be warranted. Such a comparison was not performed. However, FEHM may have more sophisticated transport capabilities with more options including two particle tracking methodologies as well as finite-element transport.

QA Evaluation

Both SWIFT-98 and FEHM have appropriate verification and validation documentation. In addition, FEHM is maintained in a software configuration management system. Both codes would receive the same ranking for the QA evaluation measure.

Ease of Use

The evaluator for SWIFT-98 described the code in [Section A.8.0](#) as difficult to use and mentioned the vagueness of the users manual. The evaluator for FEHM ([Section A.9.0](#)) found the code relatively easy to implement for this problem and the users manual helpful. However, ease of use is a subjective measure and probably provides little distinction between the codes. Based on the quality of the users manuals FEHM would be ranked slightly higher than SWIFT-98 for ease of use.

Speed of Simulation

The CPU times required by FEHM and SWIFT-98 for specific simulations are shown in [Tables A.11-2](#) and [A.11-3](#). Comparing first the time required for simulation of a steady-state flow field with the presence of faults, FEHM required 15 minutes and SWIFT-98, 23 minutes. Transport simulations were consistently faster for SWIFT-98 than for FEHM. The time required to simulate 200 years of tritium transport with faults for sources located at the working points of SCOTCH and SERENA was 64 minutes for SWIFT-98 and 77 minutes for FEHM. When the source was moved up to the CHVTA, SWIFT-98 required 58 minutes and FEHM, 103 minutes. For the simulations with time-varying fluxes the times for simulation of individual radionuclides required by SWIFT-98 must be added for comparison to the multi-species FEHM simulations. Total times required to simulate 1000 years of transport for Am-241, Pu-239, and Sr-90 with faults for sources located at the working points were 106 minutes for SWIFT-98 and 142 minutes for FEHM. When the source was moved up to the CHVTA, simulation times were 120 minutes for SWIFT-98 and 153 minutes for FEHM.

While the transport simulation times for SWIFT-98 were somewhat faster than for FEHM an additional characteristic of SWIFT-98 must be considered when evaluating the speed of simulation for the CAU modeling effort. As discussed in [Section A.8.0](#), SWIFT-98 requires that most of the solute transport parameters required for radionuclide transport in a steady-state flow field be input into the steady-state flow simulation data set. As a result, if a change is desired in the transport parameters, the flow field must be simulated again. This makes it difficult to perform multiple transport simulations based on a single steady-state flow simulation. FEHM does not have this limitation. For the Frenchman Flat CAU model, SWIFT-98 was updated to allow for changes in half-life and adsorption coefficient for each transport simulation without rerunning the flow problem. For parameters such as dispersivity the terms are assembled in conjunction with the steady-state flow run and used as composite terms thereafter (even in restart runs). Updating SWIFT-98 to reassemble the composite terms would be a more difficult procedure. With this limitation, FEHM would be ranked above SWIFT-98 for speed of simulation. If SWIFT-98 was updated to allow changes in all transport parameters without rerunning the flow problem, the rankings would be reversed.

Given the relative rankings of SWIFT-98 and FEHM for the five measures discussed above, FEHM is the code recommended for the Pahute Mesa CAU modeling effort.

A.11.0 REFERENCES

- Ashby, S.F. 1996. Par-Flow Home Page: <http://www.llnl.gov/CASC/ParFlow/>.
- Dash, Z.V., B.A. Robinson, and G.A. Zyvoloski. 1997. Software requirements, design, and verification and validation for the FEHM application - A finite-element heat- and mass-transfer code. Los Alamos National Laboratory report LA-13305-MS.
- Drellack, S.L., Jr., and L.B. Prothro. 1997. Descriptive narrative for the hydrogeologic model of Western and Central Pahute Mesa Corrective Action Units. Prepared for the U.S. Department of Energy of Energy, Nevada Operations Office. Las Vegas, NV.
- Duffield, G.M., J.J. Benegar, and D.S. Ward. 1996. MODFLOWT, A modular three-dimensional groundwater flow and transport model, user's manual version 1.1. Sterling, VA: HSI GeoTrans, Inc.
- George, D. 1997. Unstructured 3D grid toolbox for modeling and simulation. Los Alamos National Laboratory Report. LA-UR-97-3052.
- Gupta, S. 1996. CFEST, Flow and solute transport, Draft user's manual. Irvine, CA: Consultant for Environmental System Technologies (CFEST).
- HSI GeoTrans. 1998. Theory and implementation for SWIFT-98: The Sandia waste-isolation flow and transport model for fractured media. HSI GeoTrans. Sterling, VA.
- IT, see IT Corporation.
- IT Corporation. 1998. Report and analysis of the BULLION forced-gradient experiment. DOE/NV/13052-042. Prepared for the U.S. Department of Energy of Energy, Nevada Operations Office. Las Vegas, NV.
- Katyal, A.K. 1995. CSMoS online model information for BIOF&T-3D. U.S. Environmental Protection – Ada Oklahoma Laboratory. Blacksburg, VA: Draper Aden Environmental Modeling, Inc.
- Kipp, K.L., Jr. 1986. HST3D: A computer code for simulation of heat and solute transport in three-dimensional ground-water flow systems. U.S. Geological Survey Water-Resources Investigations Report 86-4095.

- Nitao, J.L. 1998. User's manual for the USNT module of the NUFT code, version 2.0. Lawrence Livermore National Laboratory report. UCRL-MA-130653.
- Pruess, K. 1991. TOUGH2 - A General Purpose Numerical Simulator for Multiphase Fluid and Heat Flow. Lawrence Berkeley Laboratory Report LBL-29400. Lawrence Berkeley Laboratory. Berkeley, CA.
- Reeves, M., D.S. Ward, N.D. Johns, and R.M. Cranwell. 1986. Theory and implementation for SWIFT II. The Sandia Waste-Isolation Flow and Transport model for fractured media. Sandia National Laboratories, NM, NUREG/CR3328.
- Scientific Software Group. 1998. Scientific Software Group Home Page: <http://www.scisoftware.com>.
- Tompson, A.F.B., C.J. Bruton, G.A. Pawloski, eds. 1999. Evaluation of the Hydrologic Source Term from Underground Nuclear Tests in Frenchman Flat at the Nevada Test Site. Lawrence Livermore National Laboratory Report UCRL-ID-132300.
- Vatnaskil Consulting Engineers. 1988. AQUA3D groundwater flow and transport model. Sudurlandsbraut 50, 108 Reykjavik, Iceland. Vatnaskil Consulting Engineers Home Page: <http://www.huglist.is/vatnaskil/index.htm>.
- Ward, D.S., M. Reeves, and L.E. Duda. 1984. Verification and field comparison of the Sandia Waste-Isolation Flow and Transport model (SWIFT), Sandia National Laboratories. Albuquerque, NM. NUREG/CR3316.
- Ward, D.S., and J. Benegar. 1998. Data input guide for SWIFT-98. The Sandia Waste-Isolation Flow and Transport model for fractured media. Release 2.57. HSI-GeoTrans. Sterling VA.
- Warren, R.G., and C.M. LaDelfe. 1991. Constraints on a basin-range fault at Pahute Mesa, Southwestern Nevada Volcanic Field. In 6th Symposium on Containment of Underground Nuclear Explosions, Conf-9109114-vol.2. C.W. Olsen, ed. Lawrence Livermore National Laboratory. Livermore, CA.
- Waterloo Hydrogeologic, Inc. 1998. FRAC3DVS: Variably-saturated groundwater flow and transport in discretely fractured porous media. Waterloo, Ontario, Canada. Waterloo Hydrogeologic Inc. Home Page: <http://www.flowpath.com>.
- Westinghouse Hanford Company. 1991. PORMC: A model for Monte Carlo simulation of fluid flow, heat, and mass transport in variably saturated geologic media. Report WHC-EP-0445. Richland, Washington.
- Zyvoloski, G.A., B.A. Robinson, Z.V. Dash, and L.L. Trease. 1997a. User's manual for the FEHM application - A finite-element heat- and mass-transfer code. Los Alamos National Laboratory report LA-13306-M.

Zyvoloski, G.A., B.A. Robinson, Z.V. Dash, and L.L. Trease. 1997b. Summary of models and methods for the FEHM application - A finite-element heat- and mass-transfer code, Los Alamos National Laboratory report LA-13307-MS.

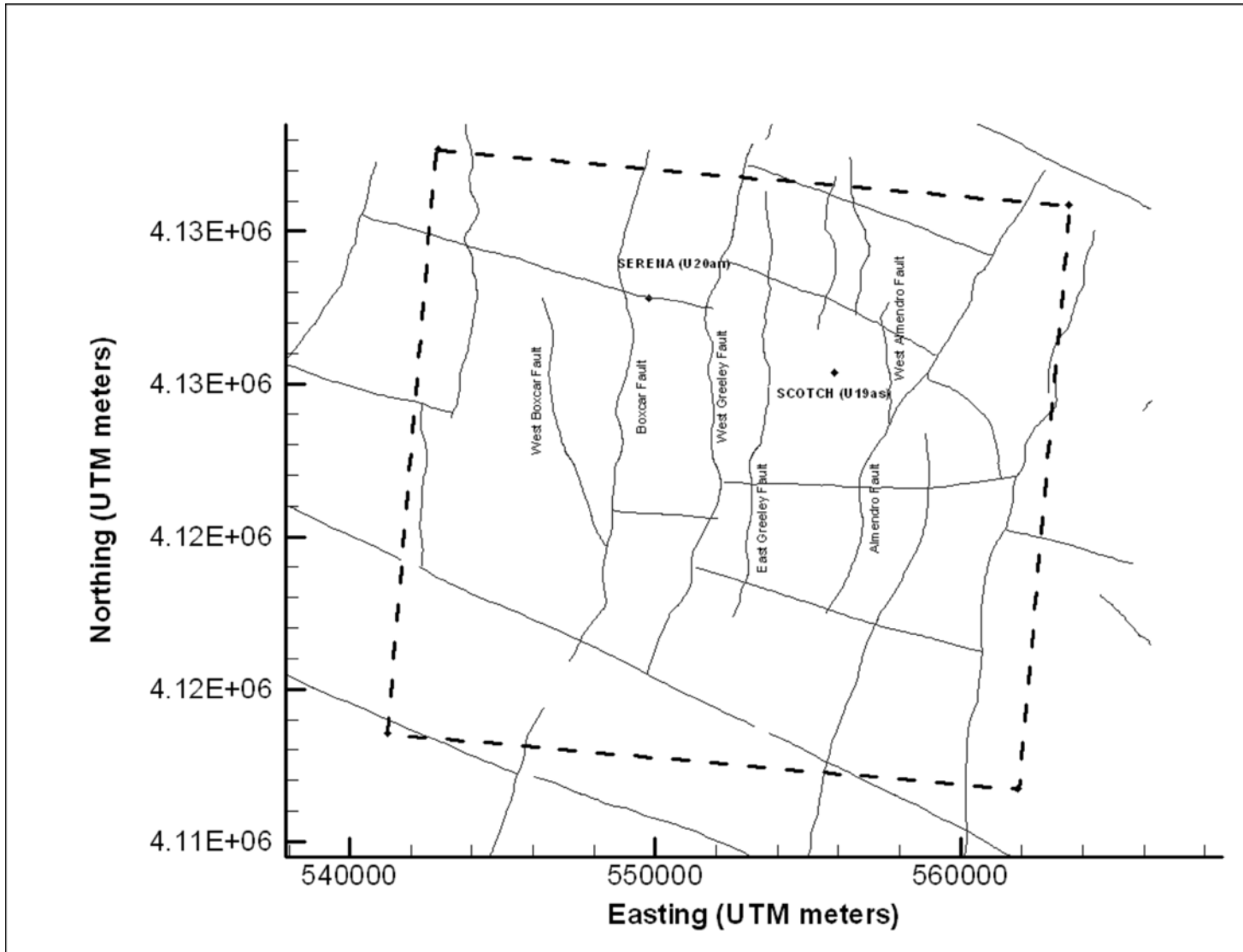


Figure A.11-1
Code Evaluation Test Problem Boundaries, Selected Faults, and Locations of SERENA (U20an) and SCOTCH (U19as) Tests

Uncontrolled When Printed

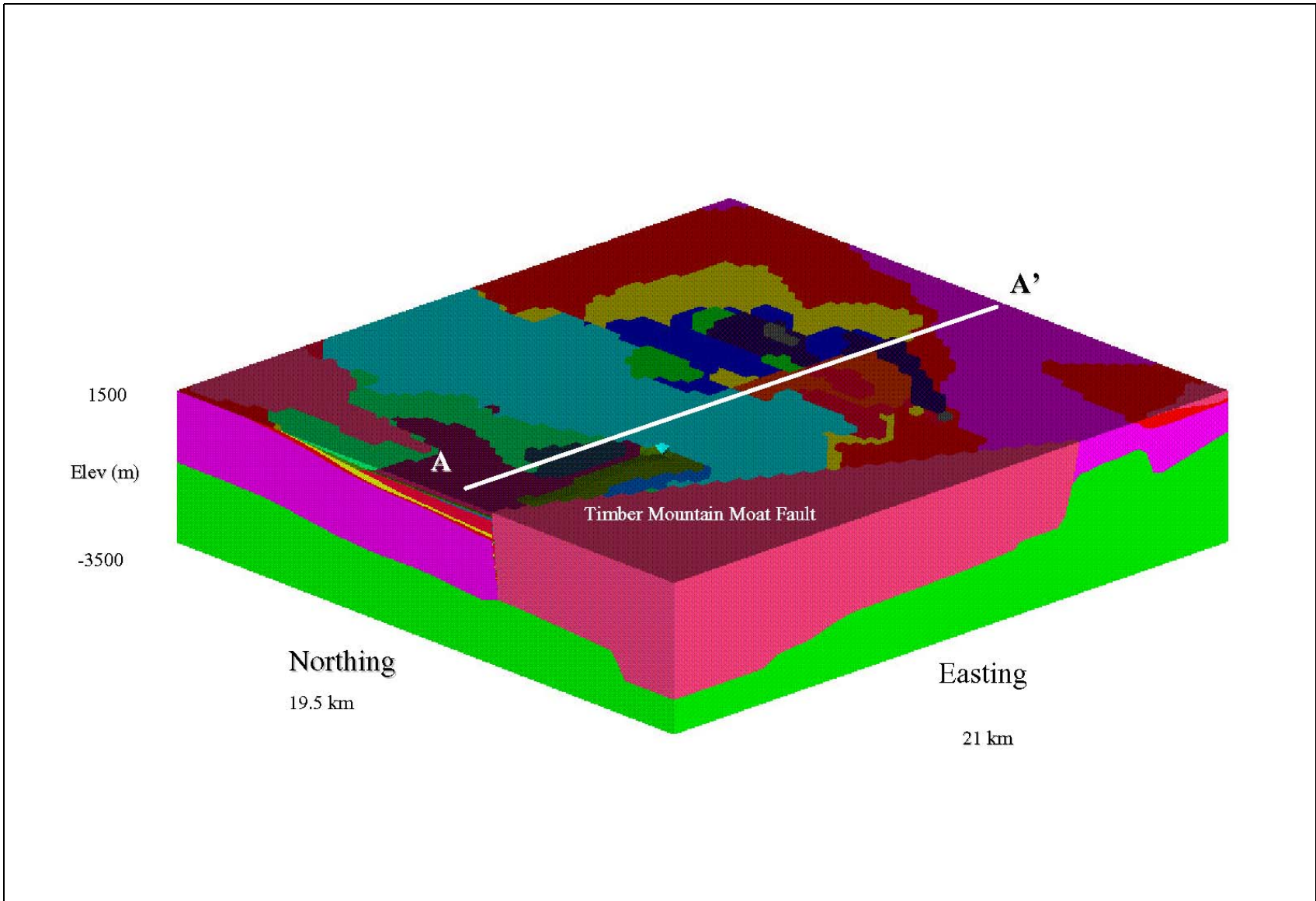


Figure A.11-2
Schematic Representation of the Three-Dimensional Hydrogeologic Model Used for the Code Evaluation Test Problem as Viewed from the Southwest Corner of the Test Problem Area

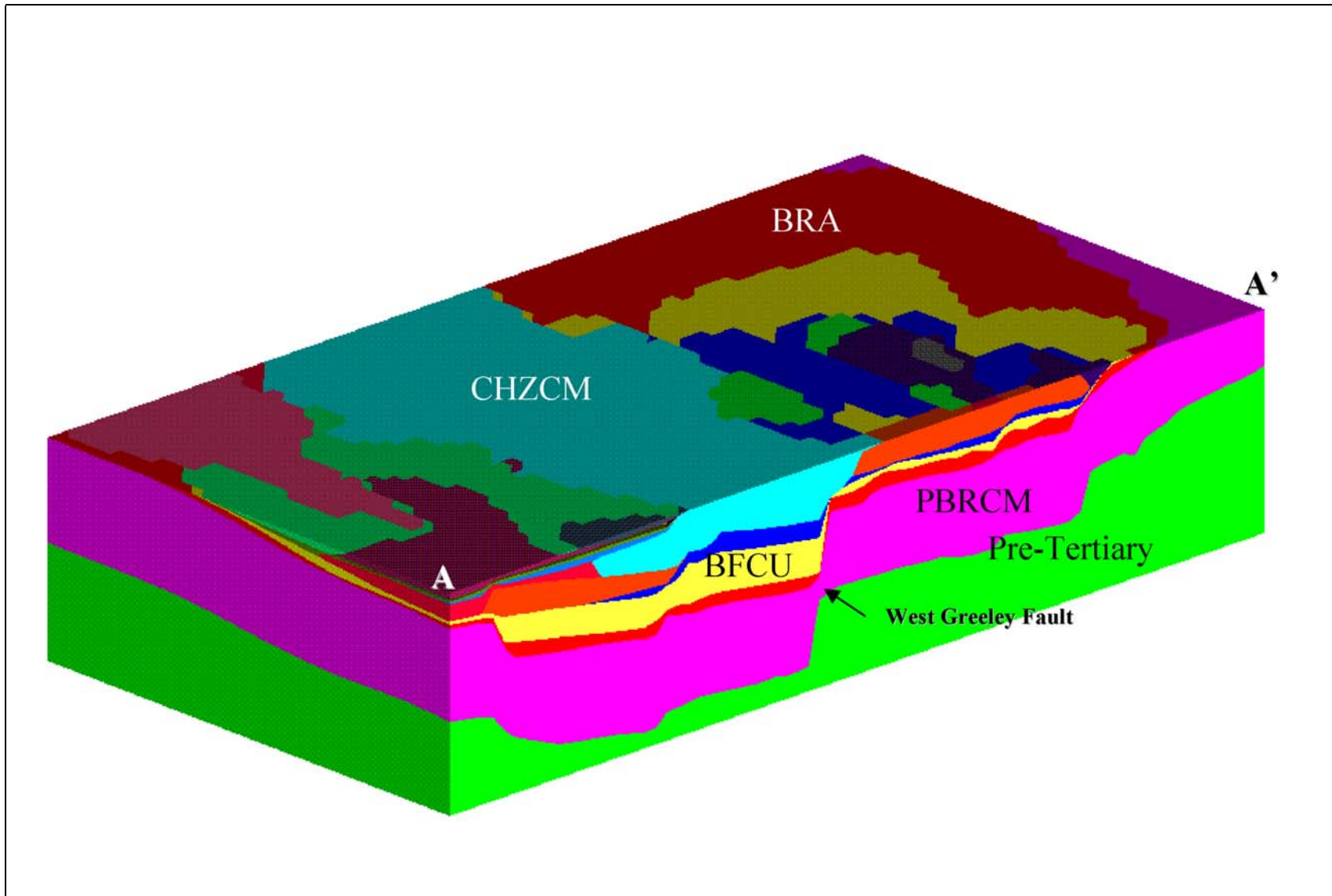


Figure A.11-3

Schematic Representation of a Cross Section Through Test Problem Domain as Viewed from the Southwest
 Units identified are Bullfrog Confining Unit (BFCU), Belted Range Aquifer (BRA), Calico Hills Zeolitized Composite Unit (CHzCM), Pre-Belted Range Composite Unit (PBRCM), and Pre-Tertiary Rocks (PreT).

Table A.11-1
Comparison of Candidate Codes by Attribute
 (Page 1 of 3)

	AQUA3D	BIOF&T-3D	CFEST	FEHM	FRAC3DVS	HST3D	MODFLOWT
Required Code Attribute							
GENERAL							
Fully three-dimensional	Y	Y	Y	Y	Y	Y	Y
500,000 nodes	?	Y	Y	Y	Y	?	Y
Transient capability	Y	Y	Y	Y	Y	Y	Y
Multiple boundary condition options	Y	Y	Y	Y	Y	Y	Y
Efficient solver	Y	Y	Y	Y	Y	?	Y
Acceptable numerical accuracy	Y	Y	Y	Y	Y	?	Y
Minimal numerical dispersion	Y	Y	Y	Y	Y	?	Y
Acceptable verification and validation	Y	Y	Y	Y	Y	?	Y
Access to source code	N	N	N	Y	Y	Y	Y
FLOW MODEL							
Saturated groundwater flow	Y	Y	Y	Y	Y	Y	Y
Heterogeneous hydraulic conductivity	Y	Y	Y	Y	Y	?	Y
Anisotropic hydraulic conductivity	Y	Y	Y	Y	Y	?	Y
Point/distributed sources/sinks of water	Y	Y	Y	Y	Y	Y	Y
Temperature dependence	Y	N	Y	Y	N	Y	N
Ability to simulate complex geology	Y	Y	Y	Y	Y	?	Y
TRANSPORT MODEL							
Advection	Y	Y	Y	Y	Y	Y	Y
Dispersion	Y	Y	Y	Y	Y	Y	Y
Sorption	Y	Y	Y	Y	Y	Y	Y
Matrix diffusion	Y	Y	N	Y	Y	N	Y
Radioactive decay	Y	Y	Y	Y	Y	Y	Y

Table A.11-1
Comparison of Candidate Codes by Attribute
 (Page 2 of 3)

	AQUA3D	BIOF&T-3D	CFEST	FEHM	FRAC3DVS	HST3D	MODFLOWT
Desirable Code Attribute							
Finite element formulation	Y	Y	Y	Y	Y	N	N
Steady state capability	N	N	N	Y	Y	?	Y
Double porosity/double permeability	N	N	N	Y	N	N	N
Multiple solutes	N	Y	?	Y	Y	N	N
Daughter products	N	Y	N	Y	Y	N	Y
Established pre- and post-processors	Y	Y	Y	Y	Y	?	Y

Y = Yes, N = No, ? = no data

	MT3D96	NUFT	PARFLOW	PORMC	SWIFT-98	TOUGH2	3DFEMFAT
Required Code Attribute							
GENERAL							
Fully three-dimensional	Y	Y	Y	Y	Y	Y	Y
500,000 nodes	Y	Y	Y	Y	Y	Y	Y
Transient capability	Y	Y	Y	Y	Y	Y	Y
Multiple boundary condition options	Y	Y	Y	Y	Y	Y	Y
Efficient solver	Y	Y	Y	Y	Y	Y	Y
Acceptable numerical accuracy	Y	Y	Y	Y	Y	Y	Y
Minimal numerical dispersion	Y	Y	Y	Y	Y	Y	Y
Acceptable verification and validation	Y	Y	Y	N	Y	Y	N
Access to source code	Y	N	Y	Y	Y	Y	N

Table A.11-1
Comparison of Candidate Codes by Attribute
 (Page 3 of 3)

Required Code Attribute	MT3D96	NUFT	PARFLOW	PORMC	SWIFT-98	TOUGH2	3DFEMFAT
FLOW MODEL							
Saturated groundwater flow	N*	Y	Y	Y	Y	Y	Y
Heterogeneous hydraulic conductivity	N*	Y	Y	Y	Y	Y	Y
Anisotropic hydraulic conductivity	N*	Y	Y	Y	Y	Y	Y
Point/distributed sources/sinks of water	N*	Y	Y	Y	Y	Y	Y
Temperature dependence	N	Y	N	Y	Y	Y	N
Ability to simulate complex geology	Y	Y	Y	Y	Y	Y	Y
TRANSPORT MODEL							
Advection	Y	Y	N	Y	Y	Y	Y
Dispersion	Y	N	N	Y	Y	N	Y
Sorption	Y	Y	N	Y	Y	N	Y
Matrix diffusion	N	Y	N	N	Y	N	N
Radioactive decay	Y	Y	N	Y	Y	N	Y
Desirable Code Attribute							
Finite element formulation	N	N	N	N	N	N	Y
Steady state capability	Y	N	N	Y	Y	N	N
Double porosity/double permeability	N	Y	N	N	N	Y	N
Multiple solutes	N	Y	N	N	N	N	N
Daughter products	Y	Y	N	N	Y	N	N
Established pre- and post-processors	Y	Y	Y	Y	Y	Y	Y

Y = Yes, N = No, ? = no data

*Transport code only. It requires specific discharge information provided by an external finite-difference code, such as MODFLOW.

Table A.11-2
CPU Times in Minutes for SWIFT-98 Test Problem Simulations

Model	Faults	Radionuclides	Source Location	Matrix Diffusion	Simulation Time (Yrs)	CPU Time (min)
Flow	No	-	-	-	-	13
Flow	Yes	-	-	-	-	23
Transport	No	Tritium	SCOTCH/SERENA*	No	200	16
Transport	No	Tritium	SCOTCH CHVTA**	No	200	54
Transport	Yes	Tritium	SCOTCH/SERENA	No	200	64
Transport	Yes	Tritium	SCOTCH CHVTA	No	200	58
Transport	No	Am	SCOTCH/SERENA	No	1000	29
Transport	No	Pu	SCOTCH/SERENA	No	1000	29
Transport	No	Sr	SCOTCH/SERENA	No	1000	31
Transport	No	Am	SCOTCH CHVTA	No	1000	29
Transport	No	Pu	SCOTCH CHVTA	No	1000	29
Transport	No	Sr	SCOTCH CHVTA	No	1000	31
Transport	Yes	Am	SCOTCH/SERENA	No	1000	29
Transport	Yes	Pu	SCOTCH/SERENA	No	1000	29
Transport	Yes	Sr	SCOTCH/SERENA	No	1000	48
Transport	Yes	Am	SCOTCH CHVTA	No	1000	29
Transport	Yes	Pu	SCOTCH CHVTA	No	1000	33
Transport	Yes	Sr	SCOTCH CHVTA	No	1000	58

*Sources were located at the SCOTCH and SERENA working points.

**Source was located in the CHVTA (Calico Hills Vitric Tuff Aquifer) above the SCOTCH working point.